

TeV Halos: Past, Present and Future

Geminga



PSR B0656+14

TIM LINDEN



- **Geminga**
 - $4.9 \times 10^{-14} \text{ TeV}^{-1} \text{ cm}^{-2} \text{ s}^{-1}$ (7 TeV)
 - $1.4 \times 10^{31} \text{ TeV s}^{-1}$ (7 TeV)
 - 25 pc extension
 - 300 kyr

Geminga

- **Monogem**
 - $2.3 \times 10^{-14} \text{ TeV}^{-1} \text{ cm}^{-2} \text{ s}^{-1}$ (7 TeV)
 - $1.1 \times 10^{31} \text{ TeV s}^{-1}$ (7 TeV)
 - 25 pc extension
 - 110 kyr

PSR B0656+14

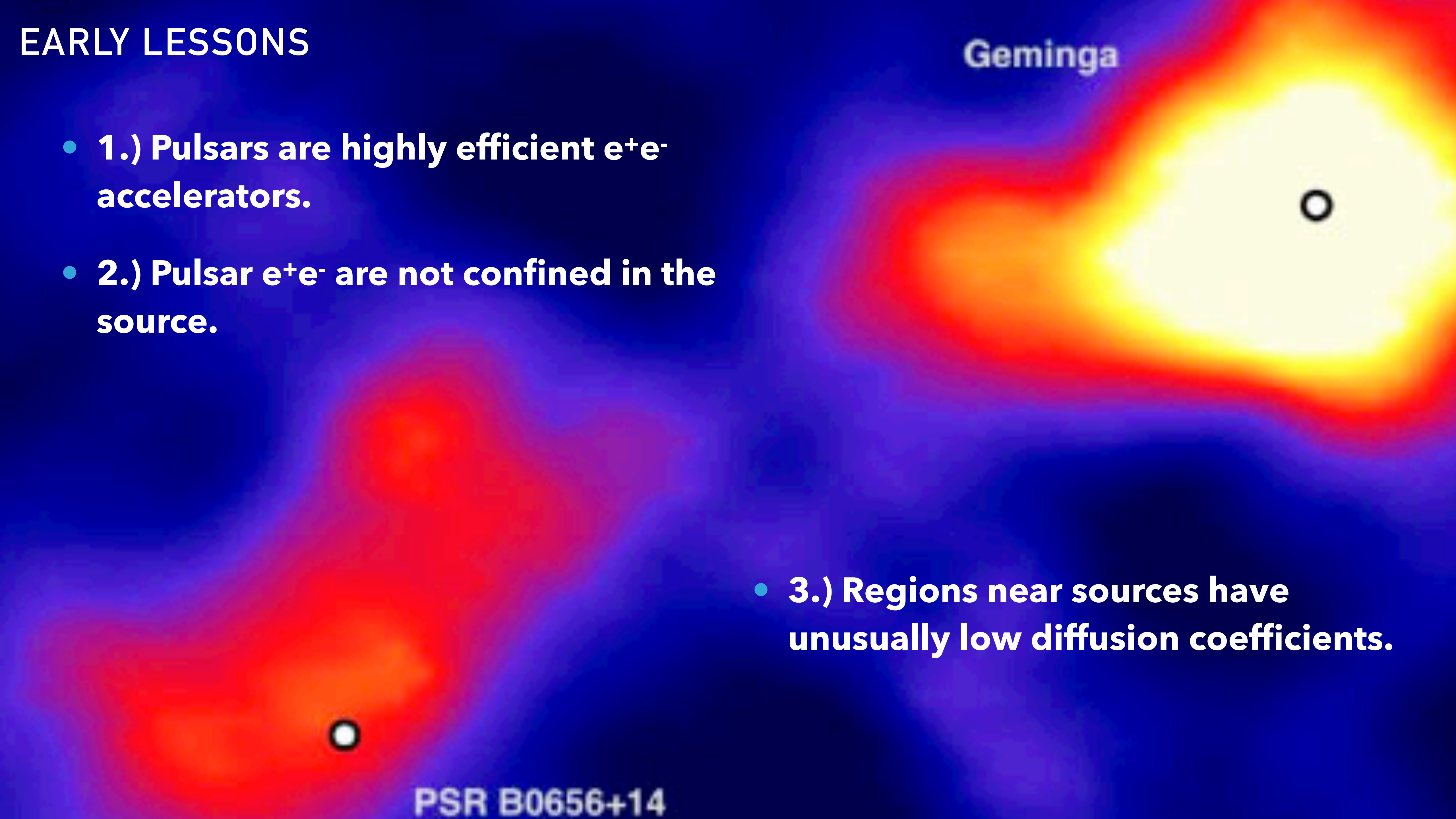
EARLY LESSONS

- 1.) Pulsars are highly efficient e^+e^- accelerators.
- 2.) Pulsar e^+e^- are not confined in the source.

Geminga

- 3.) Regions near sources have unusually low diffusion coefficients.

PSR B0656+14

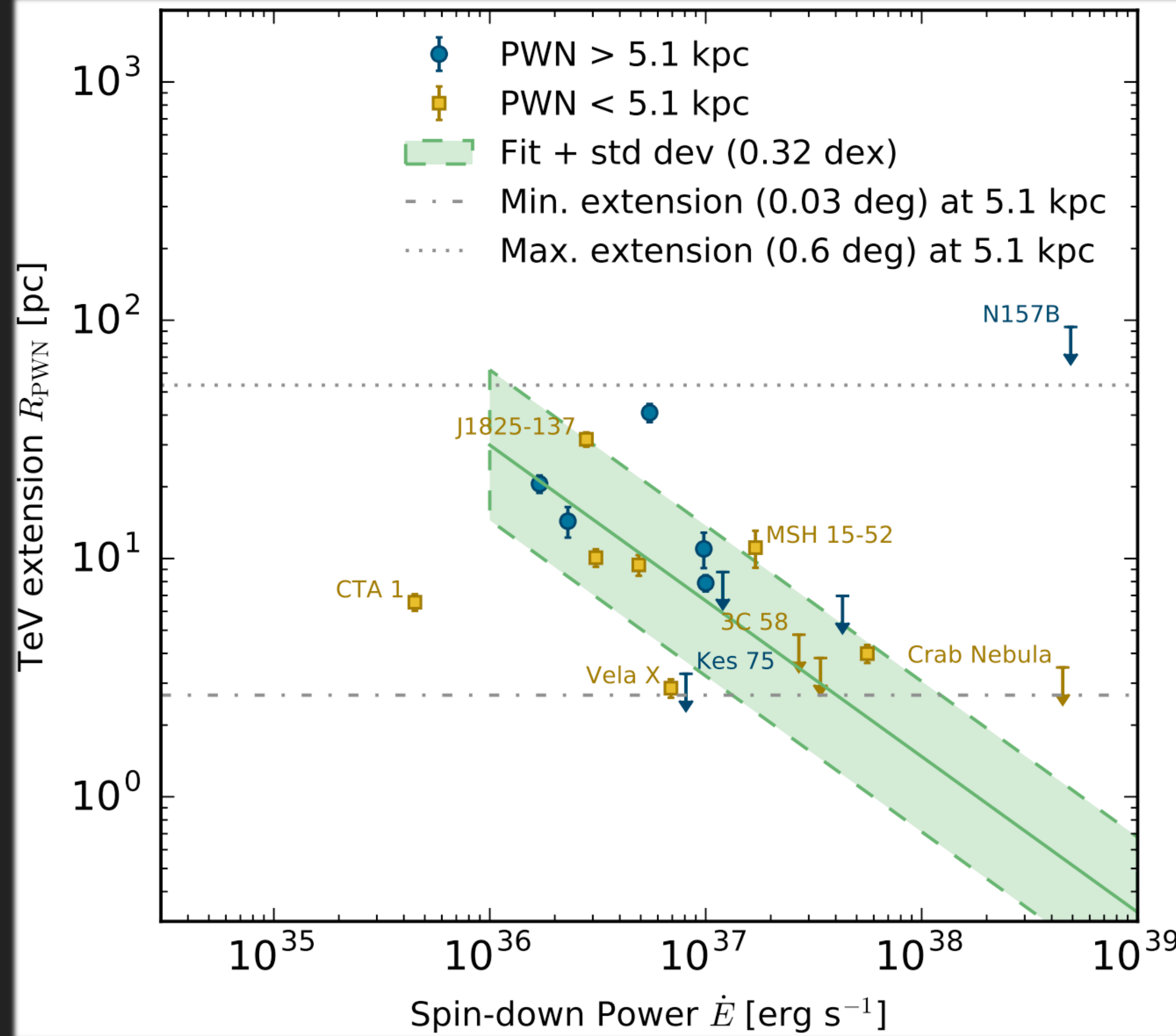


A NEW SOURCE CLASS

TeV Halos are much larger than PWN, especially at low spin down energies and large ages.

NOTE: The size of halos has the opposite time-dependence as the X-Ray PWN.

$$R_{\text{PWN}} \simeq 1.5 \left(\frac{\dot{E}}{10^{35} \text{ erg/s}} \right)^{1/2} \times \left(\frac{n_{\text{gas}}}{1 \text{ cm}^{-3}} \right)^{-1/2} \left(\frac{v}{100 \text{ km/s}} \right)^{-3/2} \text{ pc}$$



EARLY LESSONS - THE GEMINGA-CENTRIC MODEL

▶ Make One Key Assumption:

ATNF Name	Dec. (°)	Distance (kpc)	Age (kyr)	Spindown Lum. (erg s ⁻¹)	Spindown Flux (erg s ⁻¹ kpc ⁻²)	2HWC
J0633+1746	17.77	0.25	342	3.2e34	4.1e34	2HWC J0631+169
B0656+14	14.23	0.29	111	3.8e34	3.6e34	2HWC J0700+143
B1951+32	32.87	3.00	107	3.7e36	3.3e34	—
J1740+1000	10.00	1.23	114	2.3e35	1.2e34	—
J1913+1011	10.18	4.61	169	2.9e36	1.1e34	2HWC J1912+099
J1831-0952	-9.86	3.68	128	1.1e36	6.4e33	2HWC J1831-098
J2032+4127	41.45	1.70	181	1.7e35	4.7e33	2HWC J2031+415
B1822-09	-9.58	0.30	232	4.6e33	4.1e33	—
B1830-08	-8.45	4.50	147	5.8e35	2.3e33	—
J1913+0904	9.07	3.00	147	1.6e35	1.4e33	—
B0540+23	23.48	1.56	253	4.1e34	1.4e33	—

▶ The following correlation is consistent with the data.

$$\phi_{\text{TeV halo}} = \left(\frac{\dot{E}_{\text{psr}}}{\dot{E}_{\text{Geminga}}} \right) \left(\frac{d_{\text{Geminga}}^2}{d_{\text{psr}}^2} \right) \phi_{\text{Geminga}}$$

- ▶ Note: Using Monogem would increase fluxes by nearly a factor of 2. The power law of this correlation doesn't greatly affect the results.

THE KEY RESULTS - POSITRON EXCESS

- **What were the uncertainties in pulsar models?**

- **I: The e^+e^- production efficiency?**

Profumo (0812.4457); Malyshev et al. (0903.1310)

% . A quantitative discussion of plausible values for f_{e^\pm} was recently given in Ref. [38]. We shall not review their discussion here, but Ref. [38] argues (see in particular their very informative App. B and C) that in the context of a standard model for the pulsar wind nebulae, a reasonable range for f_{e^\pm} falls between 1% and 30%.

- **II: The e^+e^- spectrum.**

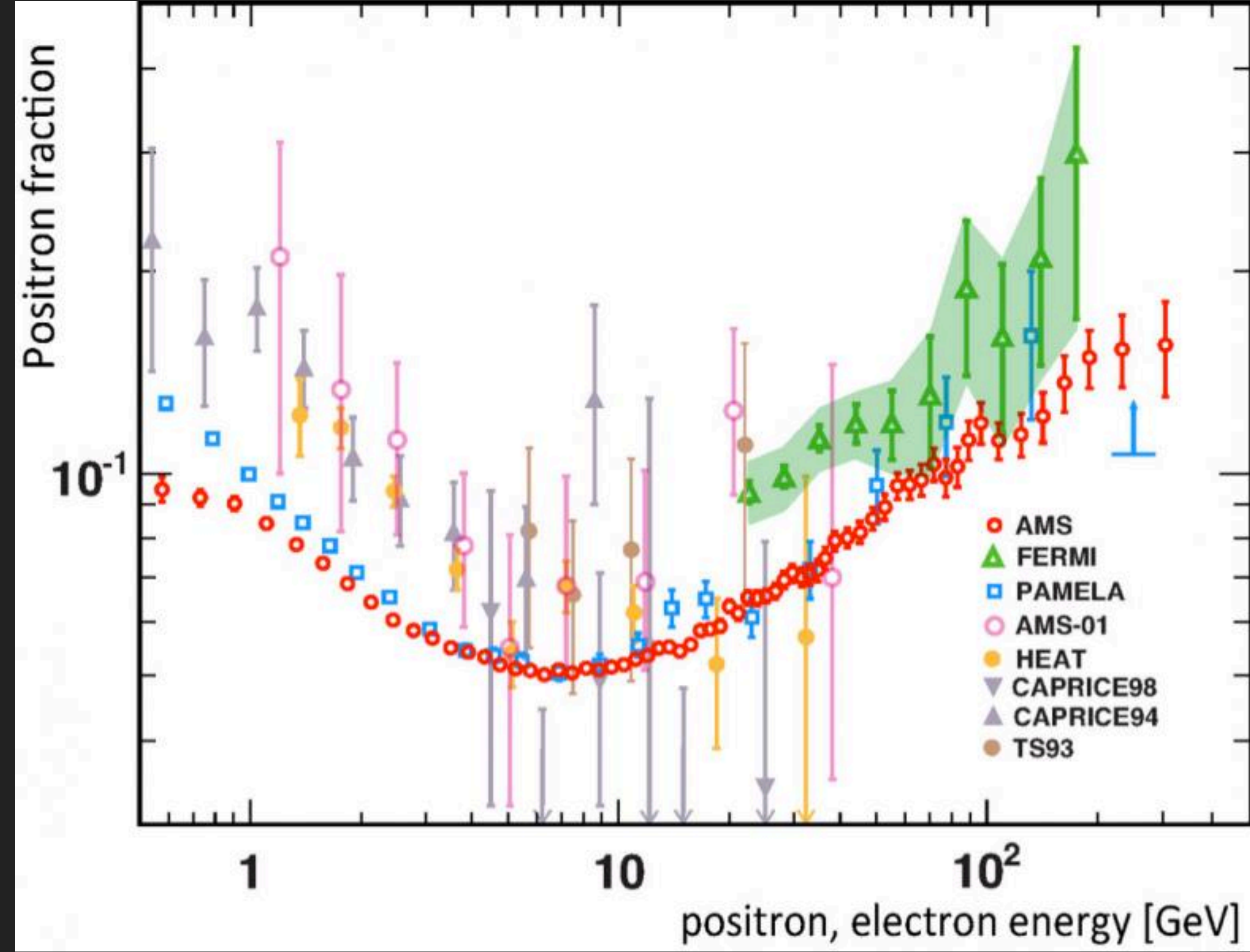
Hooper et al. (0810.1527)

part of their energy adiabatically because of the expansion of the wind. The energy spectrum injected by a single pulsar depends on the environmental parameters of the pulsar, but some attempts to calculate the average spectrum injected by a population of mature pulsars suggest that the spectrum may be relatively hard, having a slope of $\sim 1.5-1.6$ [18]. This spectrum, however, results from a complex interplay of individual pulsar spectra, of the spatial and age distributions of pulsars in the Galaxy, and on the assumption that the chief channel for pulsar spin down is magnetic dipole radiation. Due to the related uncertainties, variations from this injection spectra cannot be ruled out. Typically, one concentrates the attention on pulsars of age $\sim 10^5$ years because younger pulsars are likely to still

- **III: The propagation of e^+e^- to Earth.**

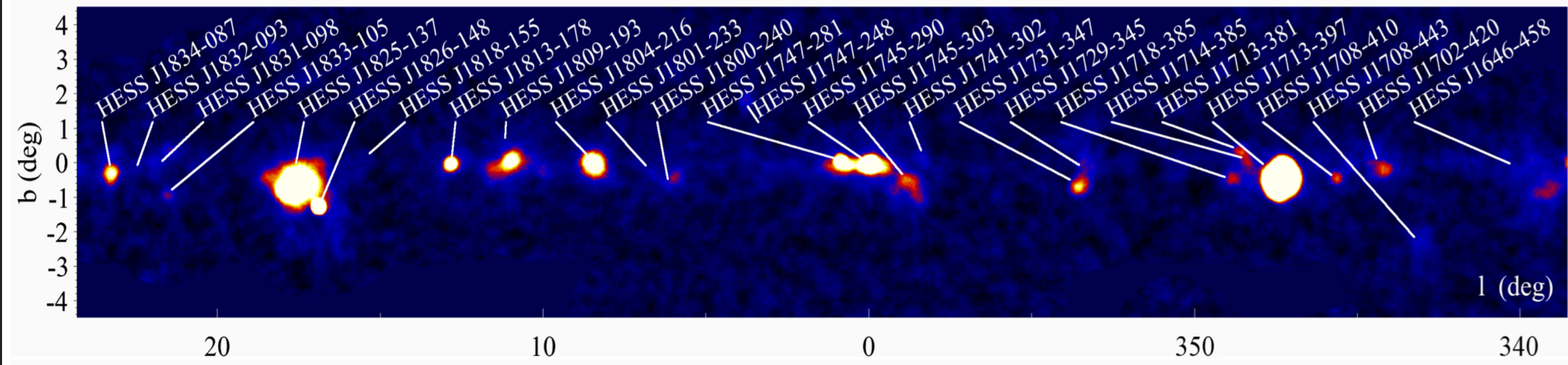
Malyshev et al. (0903.1310)

The observed spectrum on Earth of electrons and positrons injected by pulsars is also strongly dependent on propagation effects. In particular, the observed cutoff in the flux of electrons from a pulsar can be much smaller than the injection cutoff due to energy losses (“cooling”) during propagation. We define the cooling break, $E_{br}(t)$, as the maximal energy electrons can have after propagating for time t . Since – as stated above – the typical



THE KEY RESULTS - MISSING TEV HALOS

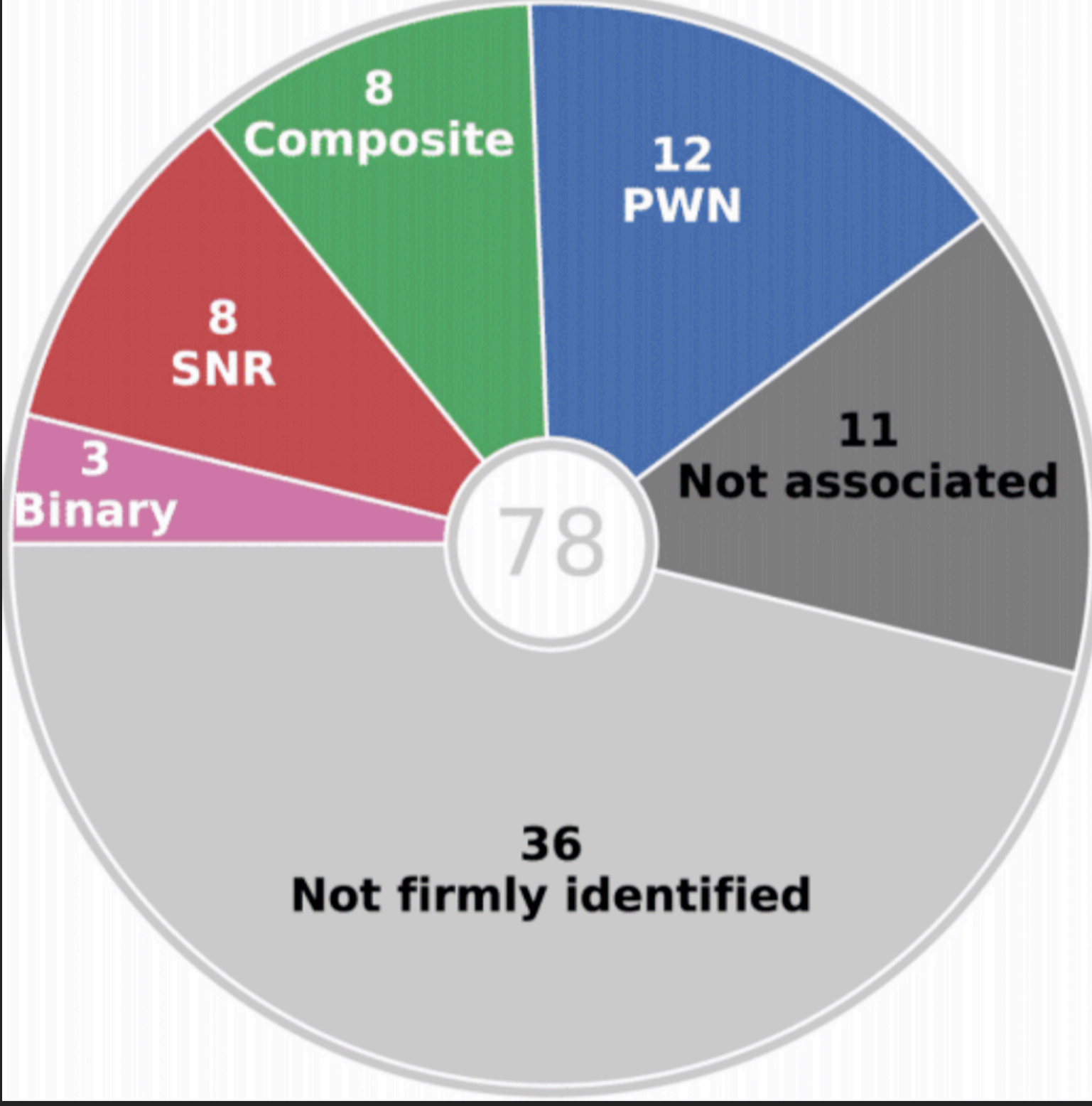
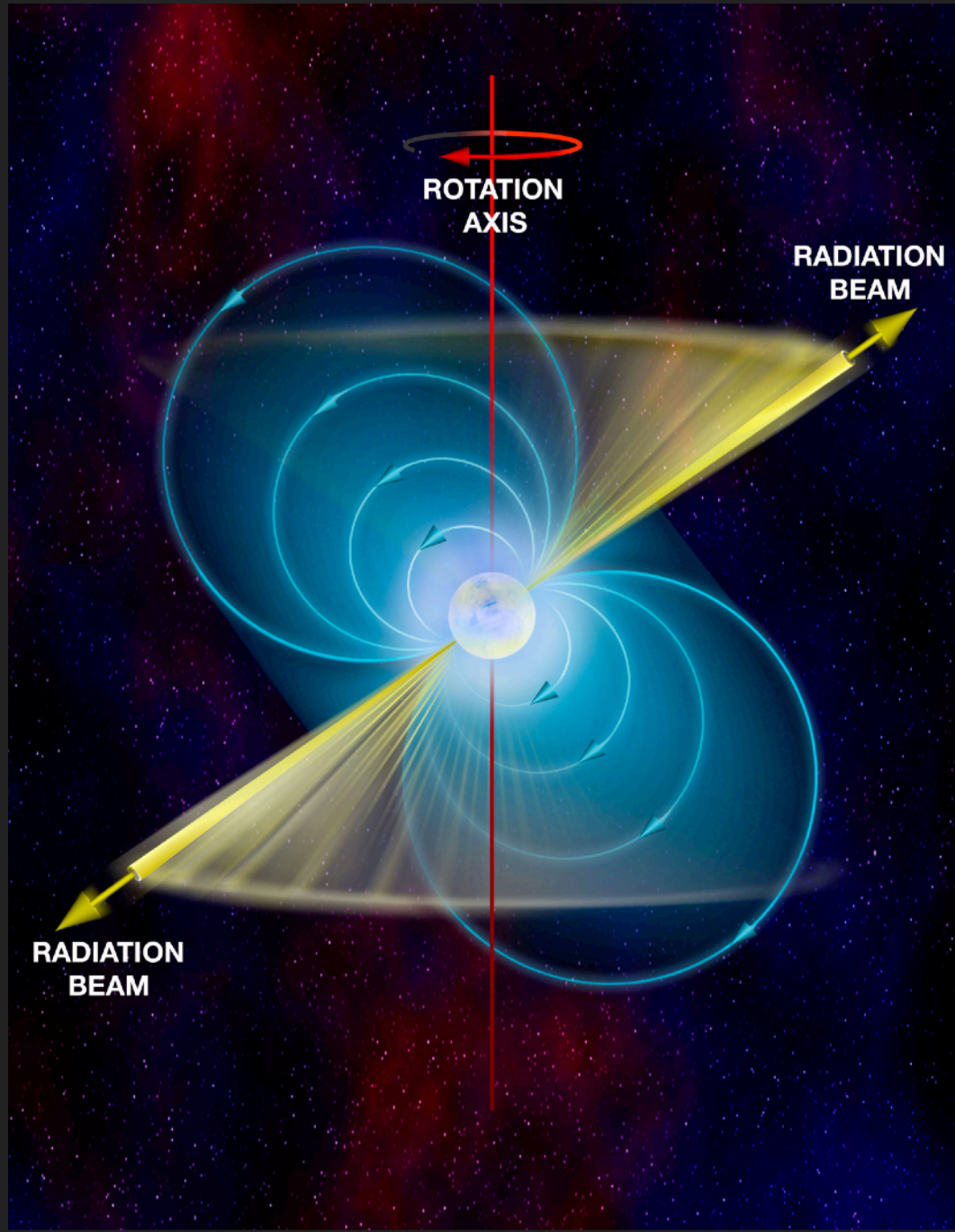
- ▶ Radio pulsars are beamed!
- ▶ Beaming fraction is small



Tauris & Manchester (1998)

$$f = \left[1.1 \left(\log_{10} \left(\frac{\tau}{100 \text{ Myr}} \right) \right)^2 + 15 \right] \%$$

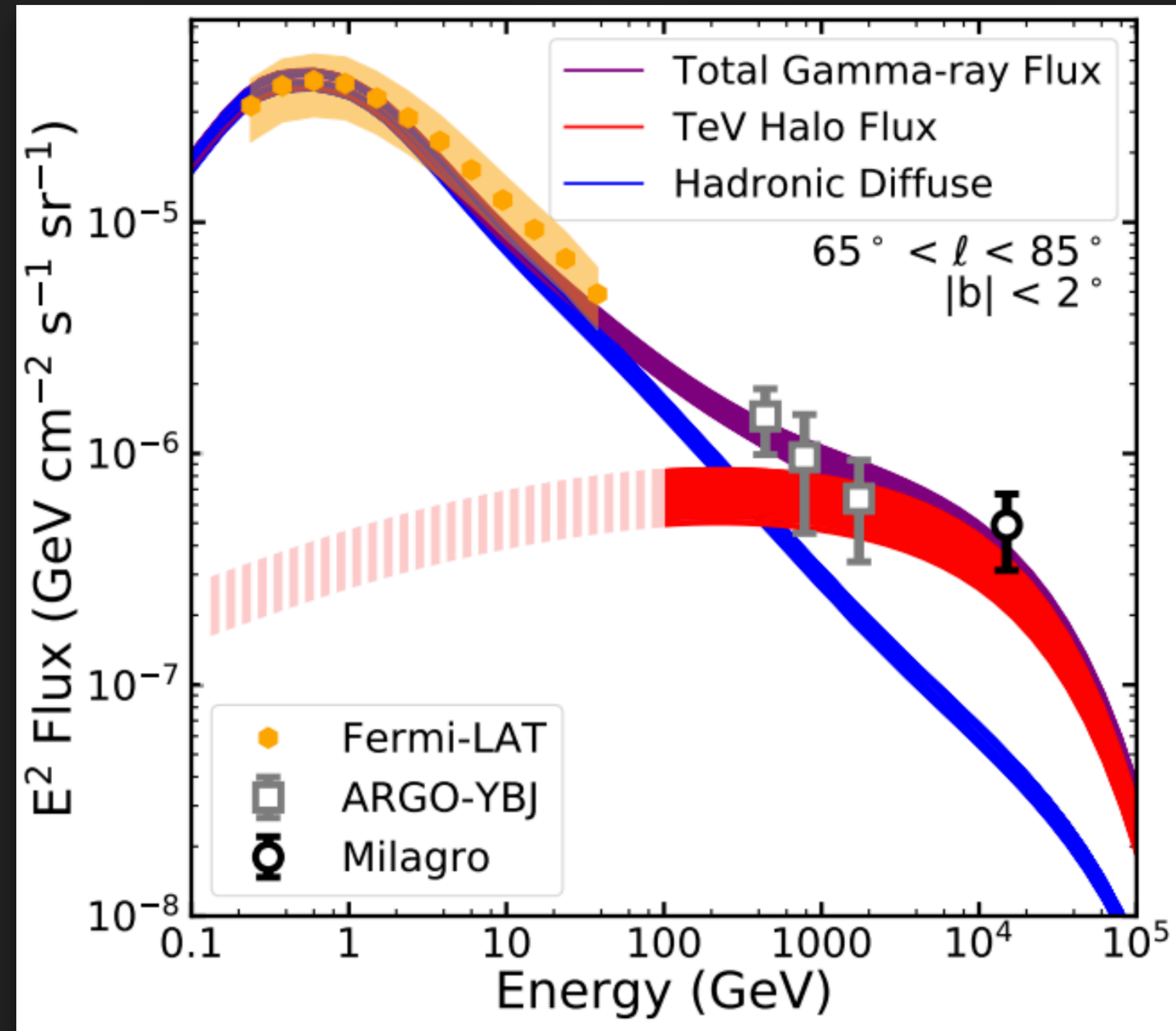
- ▶ This varies between 15-30%.
- ▶ Most pulsars are unseen in radio!



THE KEY RESULTS - DIFFUSE TEV EMISSION

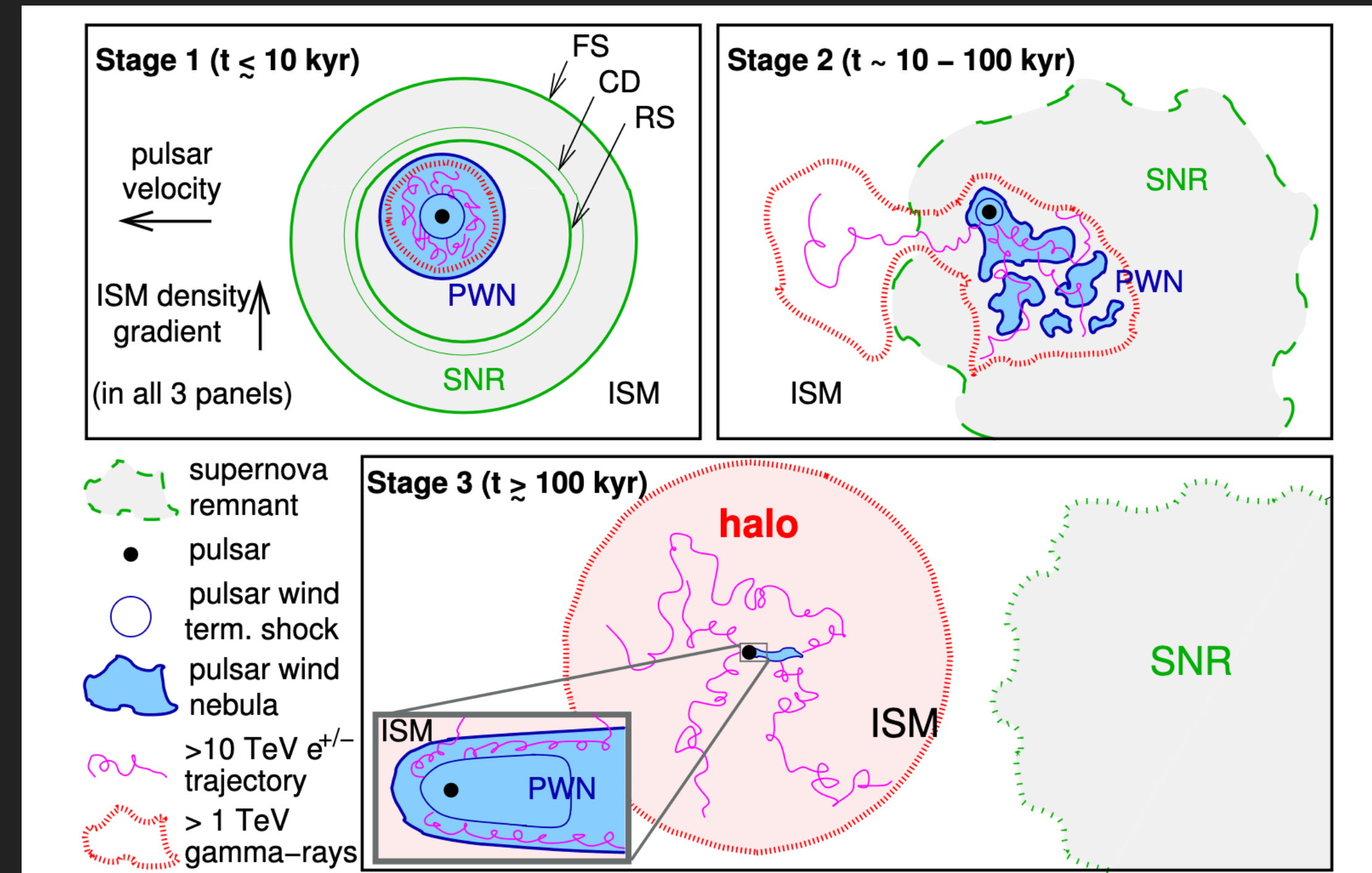
Linden & Buckman (2017; 1707.01905)

- If all convert a similar fraction of their spin down power to e^+e^- pairs as Geminga, then TeV halos naturally explain this observation.
- Note - "Halo" is not needed
 - Pulsar efficiency $\sim 10\%$
 - Power must escape PWN



DIFFERENCES IN DEFINITION - GOING BEYOND THE GEMINGA-MODEL

- An alternative definition of a “TeV halo” is used by Giacinti et al. 2019 (1907.12121)
- Linden et al. (2017) - A TeV halo is a leptonic gamma-ray source surrounding a pulsar, where the electrons are diffusing through the medium (rather than being driven by convective pulsar winds).
- Giacinti et al. (2019) - A TeV halo is a leptonic gamma-ray source surrounding a pulsar, where the emission stems from a region where the electron density falls below the ambient ISM electron density.

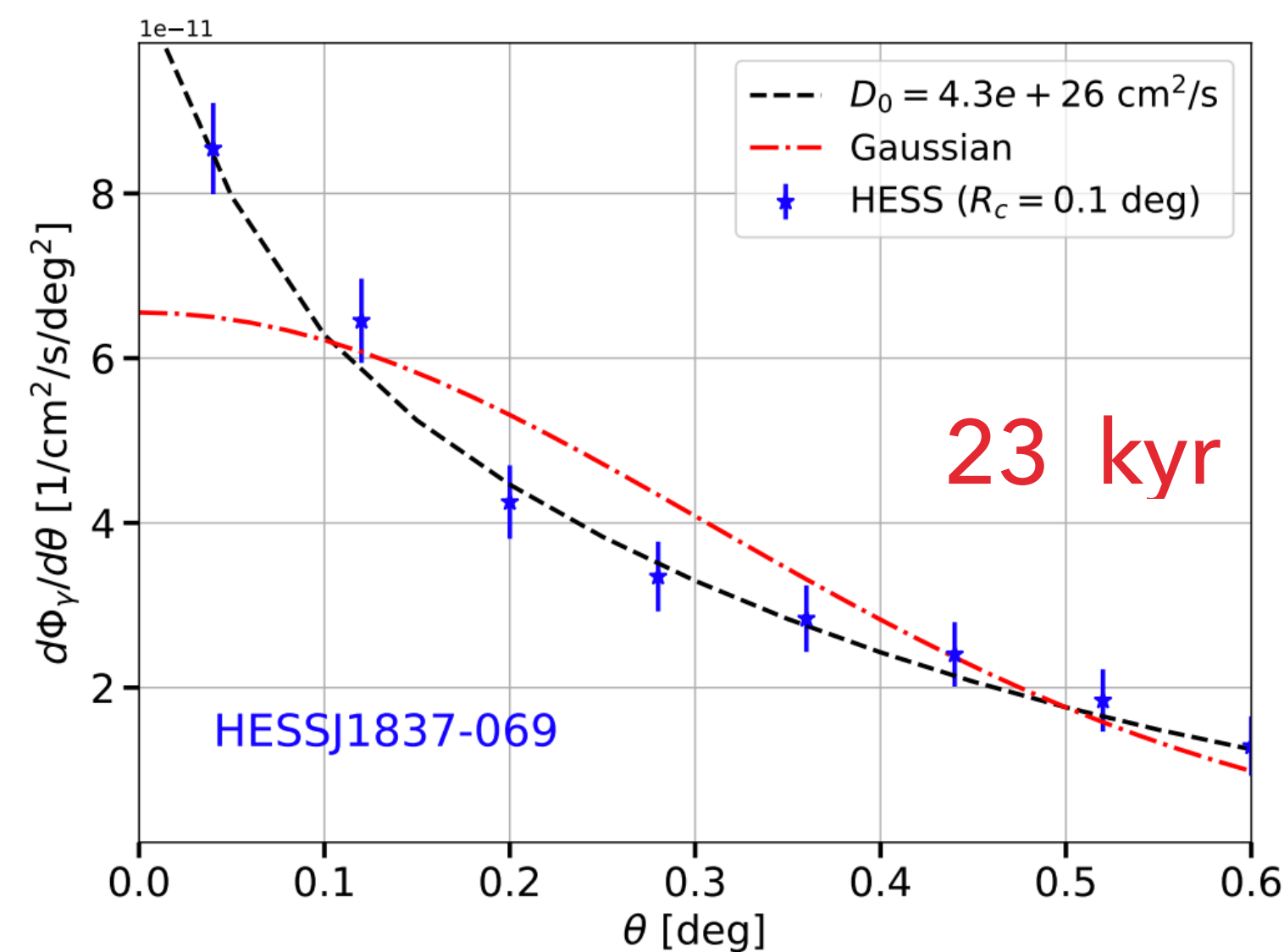
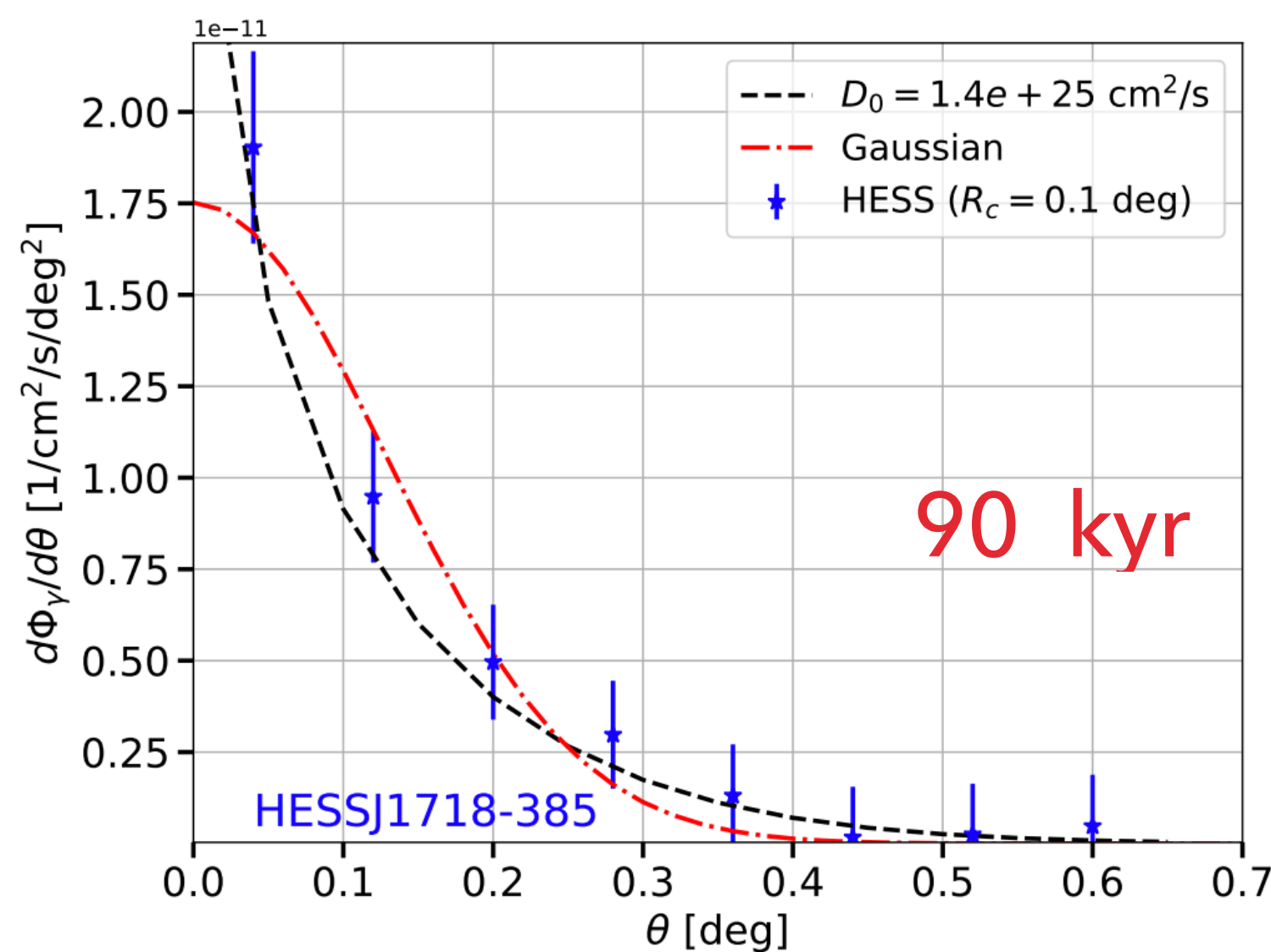
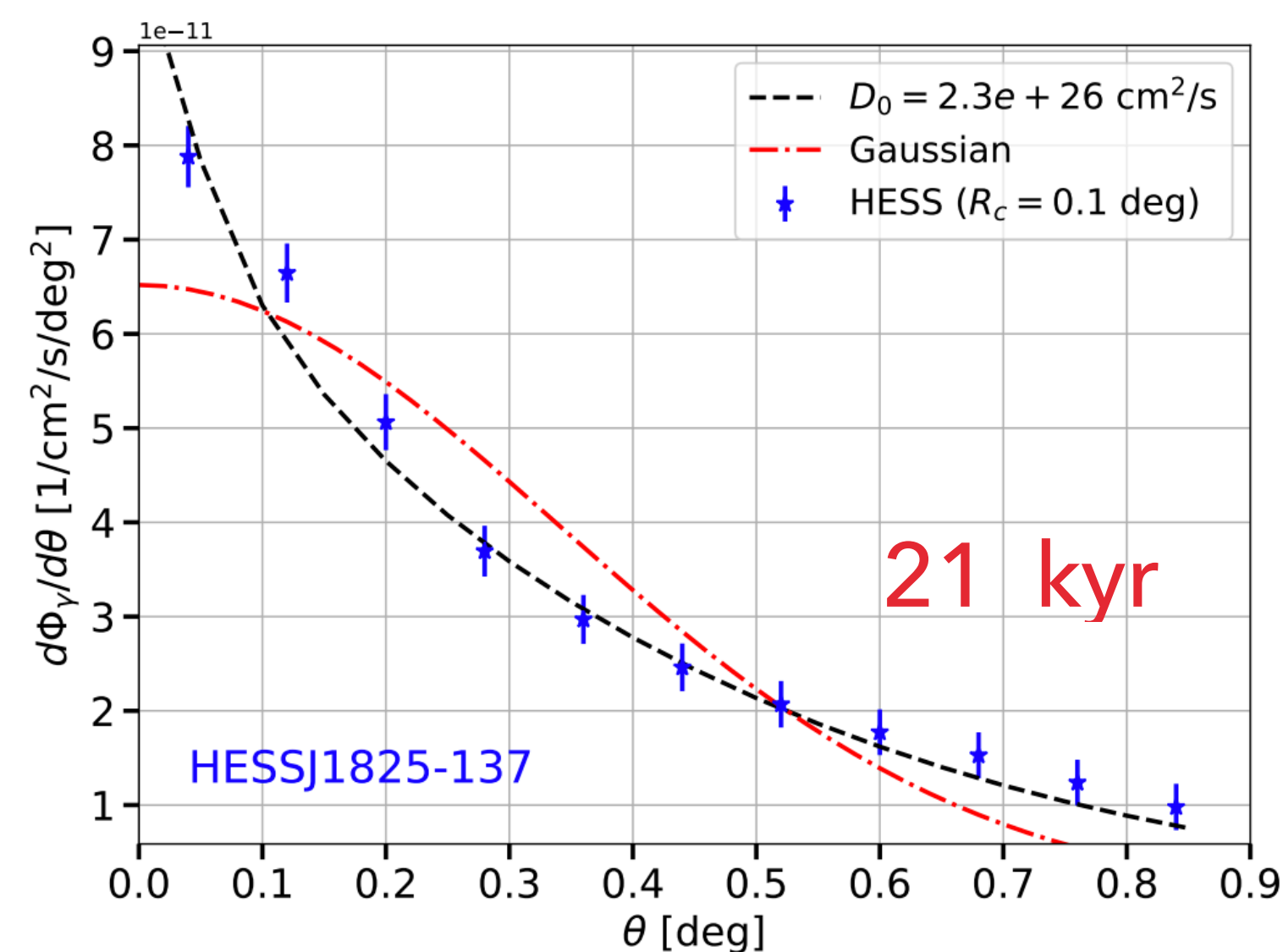
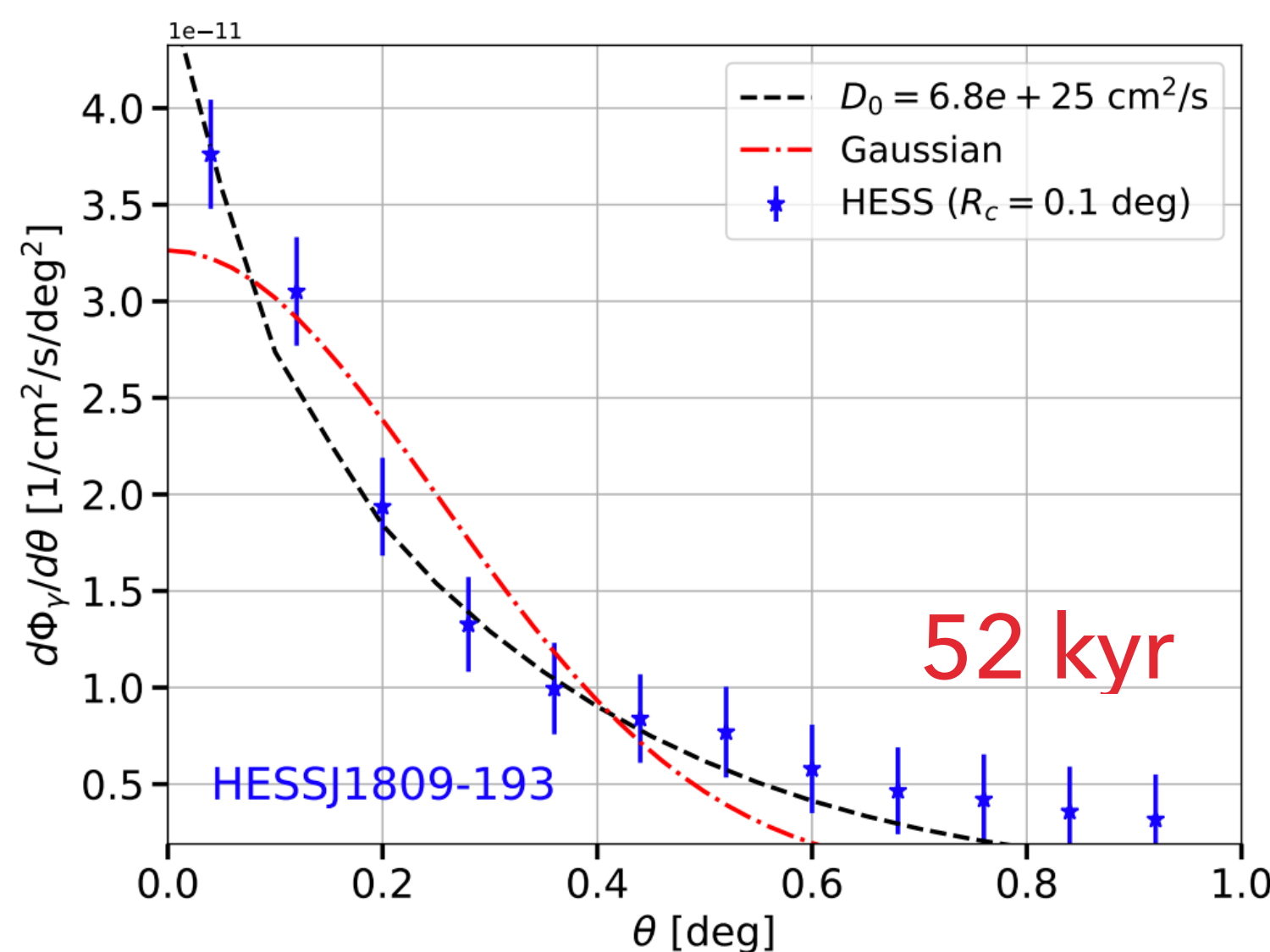


ADOPTING A MAXIMALIST VERSION OF TEV HALOS - OBSERVATIONS

Di Mauro, Manconi, Donato (2019; 1908.03216)

► In particular, this extended diffusive halos have been found in a number of young systems.

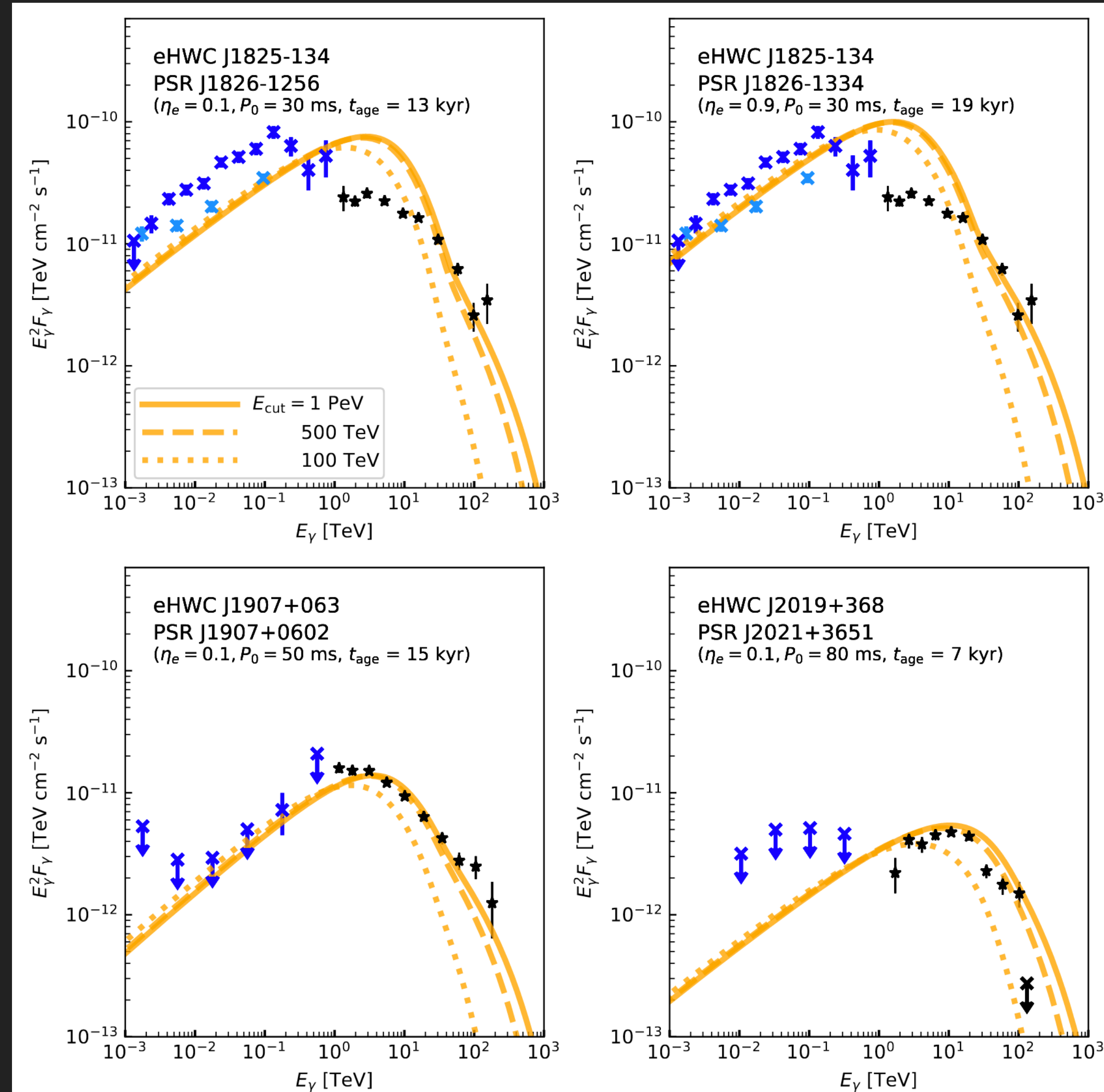
► Inhibited diffusion appears to occur very soon after system formation, and persist for a long time.



ADOPTING A MAXIMALIST VERSION OF TEV HALOS - OBSERVATIONS

Sudoh, Linden, Hooper (2101.11026)

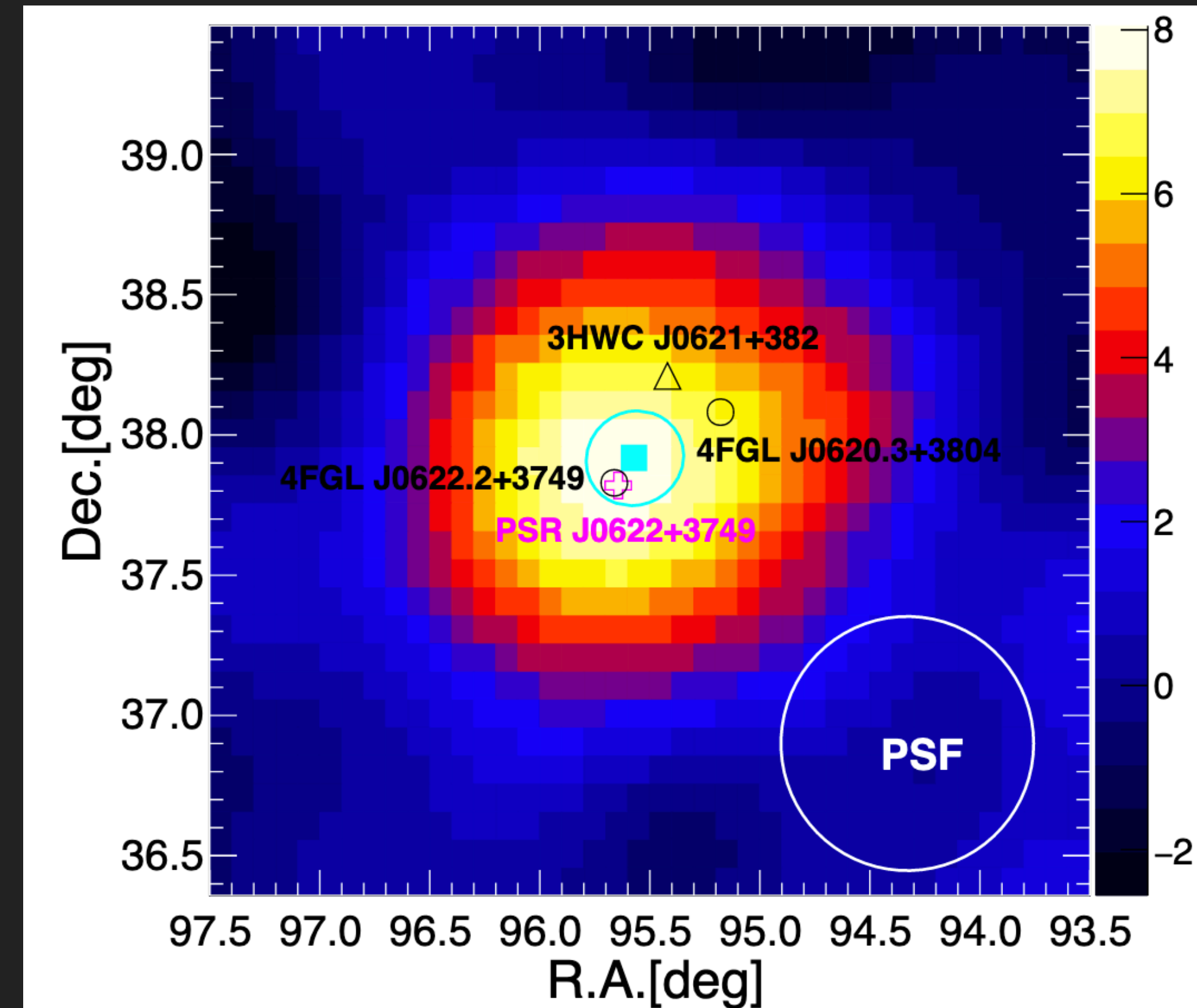
- ▶ 8 out of the 9 HAWC sources observed above 56 TeV are consistent with the location of young pulsars.
- ▶ Likely PWN or composite objects – but TeV halo contributions must be carefully examined.



ADOPTING A MAXIMALIST VERSION OF TEV HALOS - OBSERVATIONS

▶ TeV Halos (Observationally):

- ▶ Detected by all instruments (HAWC, LHAASO, HESS, VERITAS)
- ▶ Currently just the tip of the Iceberg: Detected systems are nearby, or have high spin down power.

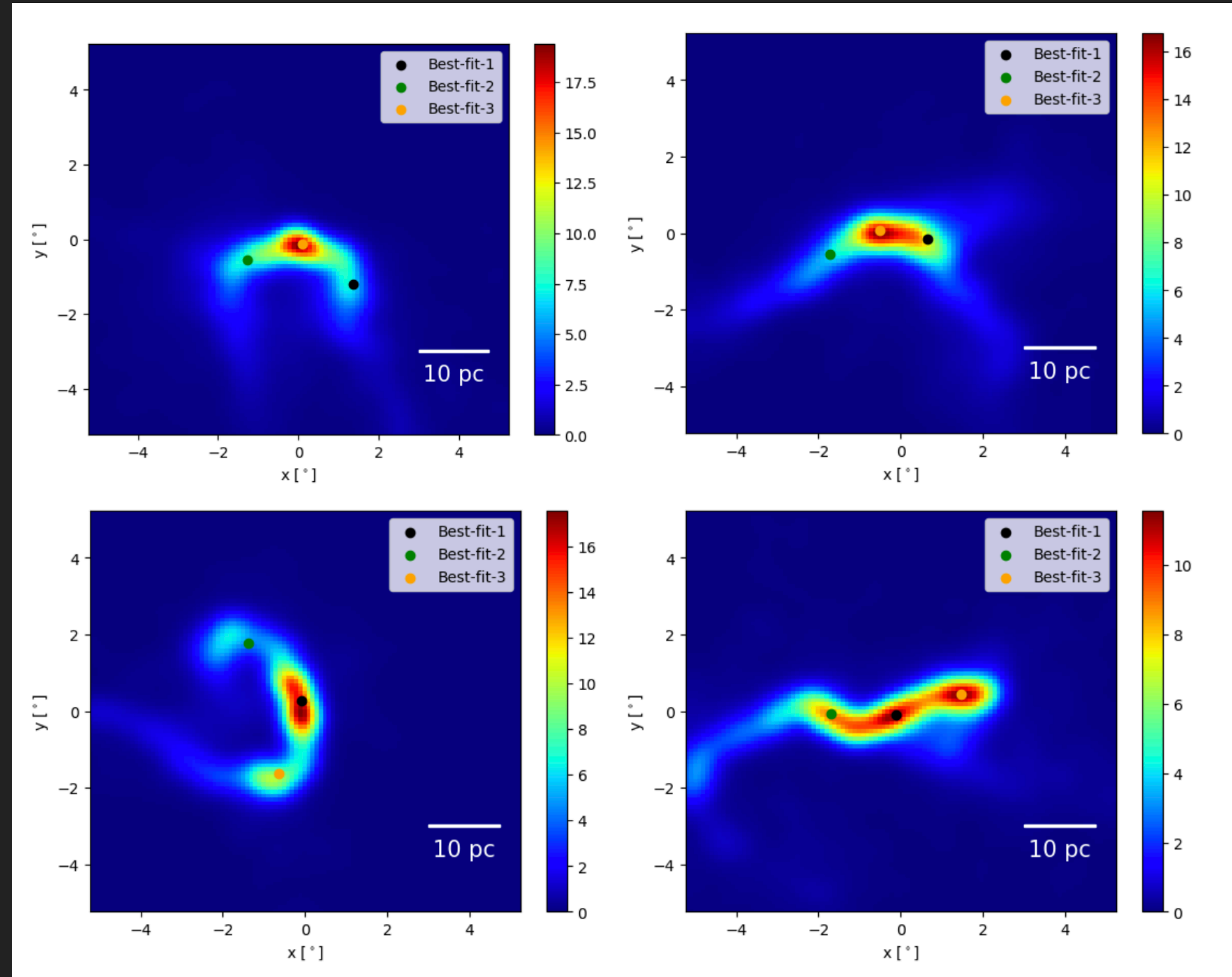


ATNF Name	Dec. (°)	Distance (kpc)	Age (kyr)	Spindown Lum. (erg s^{-1})	Spindown Flux ($\text{erg s}^{-1} \text{kpc}^{-2}$)	2HWC
J0633+1746	17.77	0.25	342	3.2×10^{34}	4.1×10^{34}	2HWC J0631+169
B0656+14	14.23	0.29	111	3.8×10^{34}	3.6×10^{34}	2HWC J0700+143
B1951+32	32.87	3.00	107	3.7×10^{36}	3.3×10^{34}	—
J1740+1000	10.00	1.23	114	2.3×10^{35}	1.2×10^{34}	—
J1913+1011	10.18	4.61	169	2.9×10^{36}	1.1×10^{34}	2HWC J1912+099
J1831-0952	-9.86	3.68	128	1.1×10^{36}	6.4×10^{33}	2HWC J1831-098
J2032+4127	41.45	1.70	181	1.7×10^{35}	4.7×10^{33}	2HWC J2031+415
B1822-09	-9.58	0.30	232	4.6×10^{33}	4.1×10^{33}	—
B1830-08	-8.45	4.50	147	5.8×10^{35}	2.3×10^{33}	—
J1913+0904	9.07	3.00	147	1.6×10^{35}	1.4×10^{33}	—
B0540+23	23.48	1.56	253	4.1×10^{34}	1.4×10^{33}	—

ADOPTING A MAXIMALIST VERSION OF TEV HALOS - OBSERVATIONS

- ▶ “Mirage” sources
 - ▶ Anisotropic diffusion can produce sources that have extremely long tails.
 - ▶ Offset from pulsar position
- ▶ Can be difficult to detect and categorize, or associate with a known pulsar.

Tentative evidence of “Mirage” sources in LHAASO catalogs!

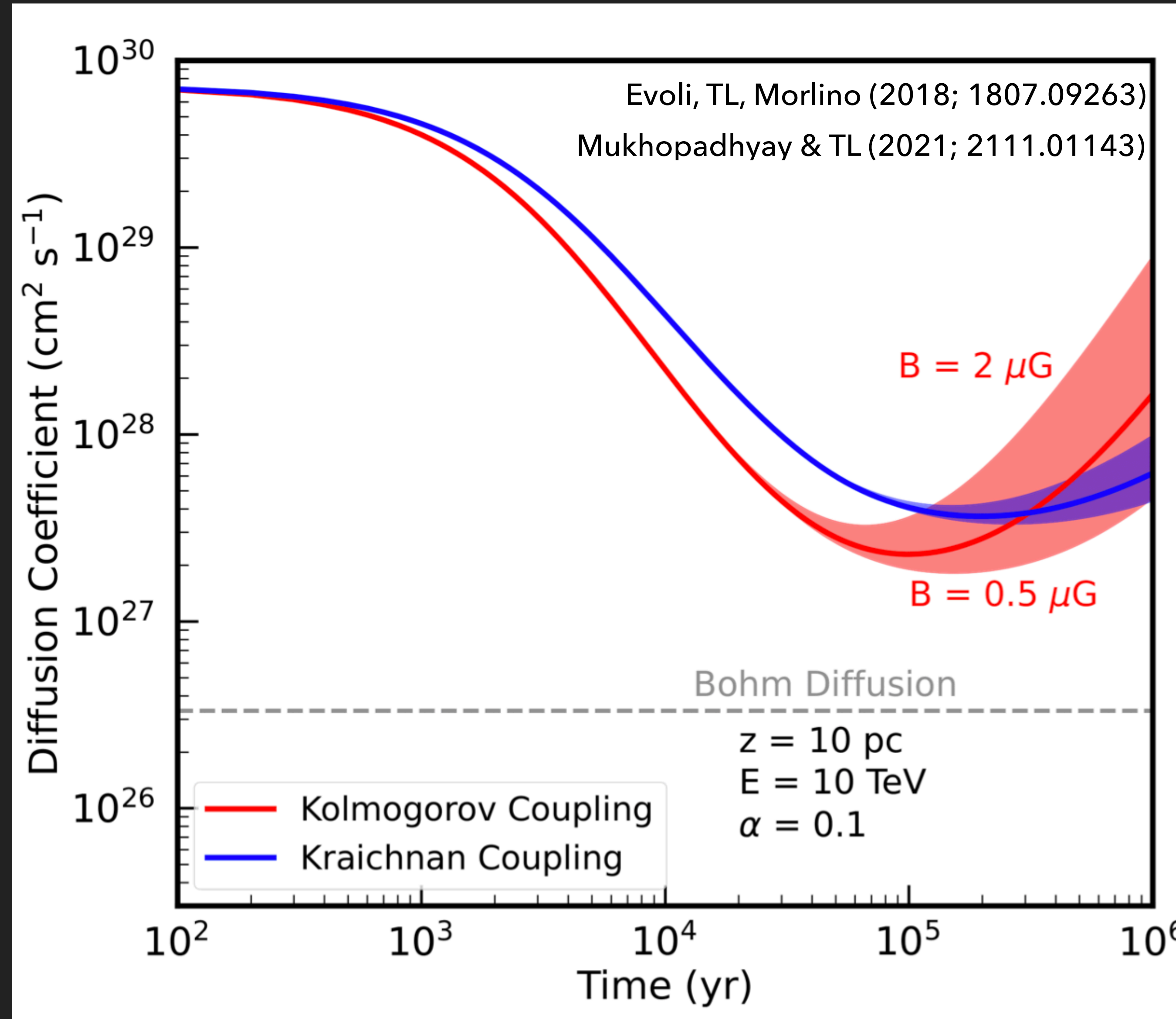


ADOPTING A MAXIMALIST VERSION OF TEV HALOS - THEORY

- ▶ Self-confinement models (and most other models for inhibited diffusion) - require the high energy of a very young pulsar.
- ▶ Probing the diffusion around the youngest systems is critical for understanding TeV halo dynamics.

$$\frac{\partial \mathcal{W}}{\partial t} + v_A \frac{\partial \mathcal{W}}{\partial z} = (\Gamma_{\text{CR}} - \Gamma_{\text{D}}) \mathcal{W}(k, z, t)$$

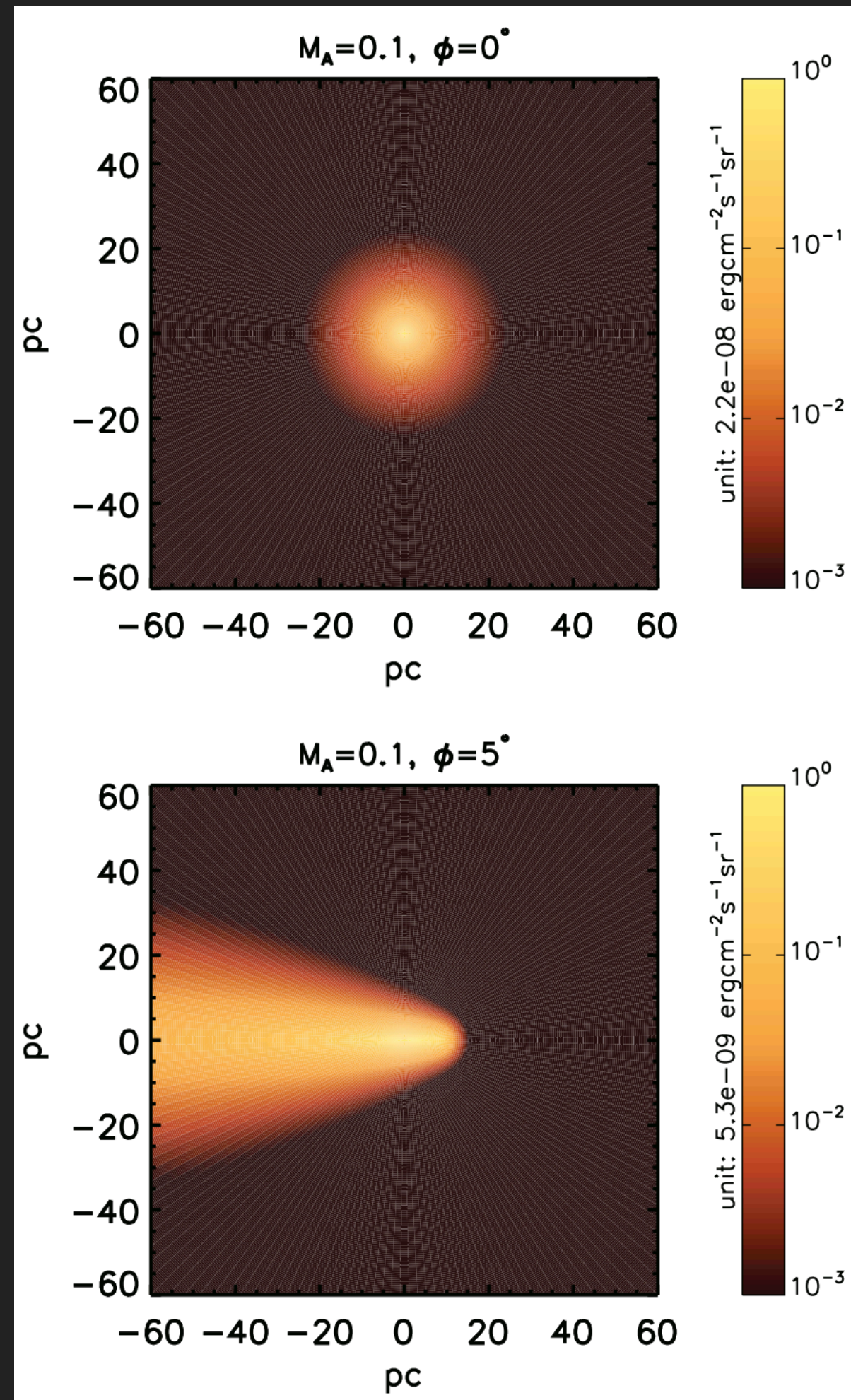
$$\Gamma_{\text{CR}}(k) = \frac{2\pi}{3} \frac{c|v_A|}{k\mathcal{W}(k)U_0} \left[p^4 \frac{\partial f}{\partial z} \right]_{p_{\text{res}}}$$



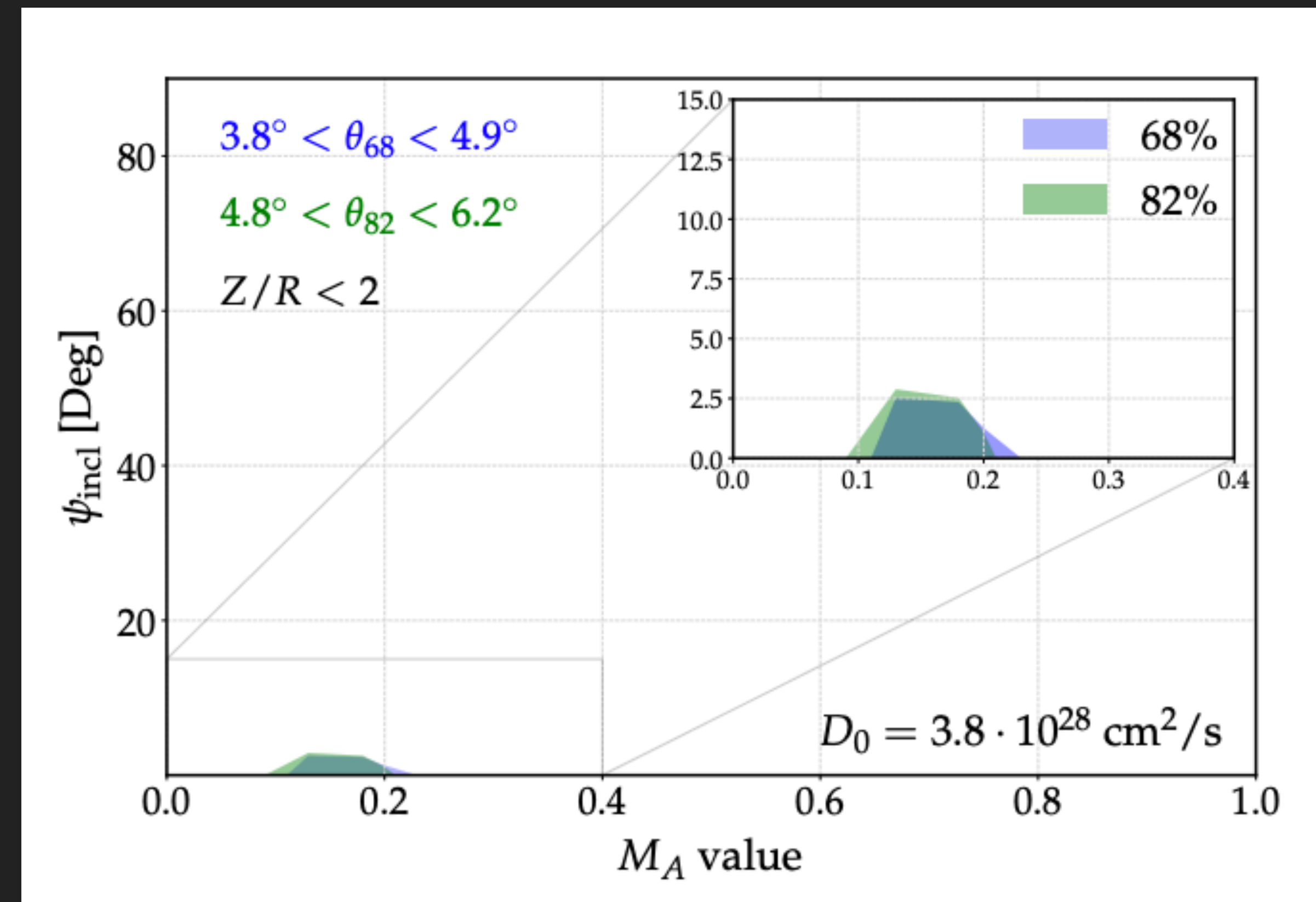
THE PRESENT: UNDERSTANDING DIFFUSION IN TEV HALOS

- ▶ By combining the large number of TeV halo observations along with energetic considerations – we know that local diffusion must be inhibited.

Liu, Yan, Zhang (2019; 1904.11536)



De la Torre Luque et al. (2022; 2205.08544)

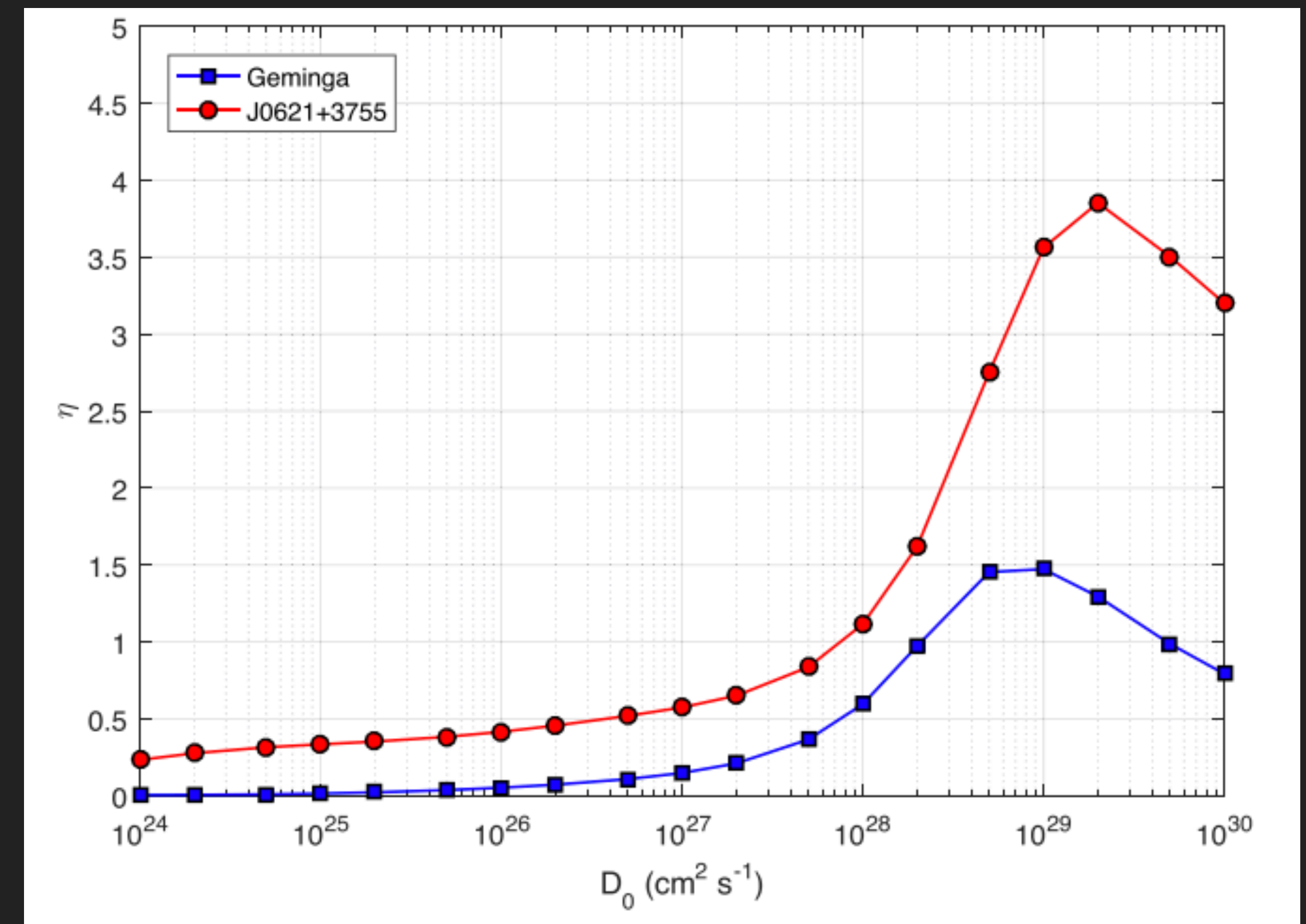
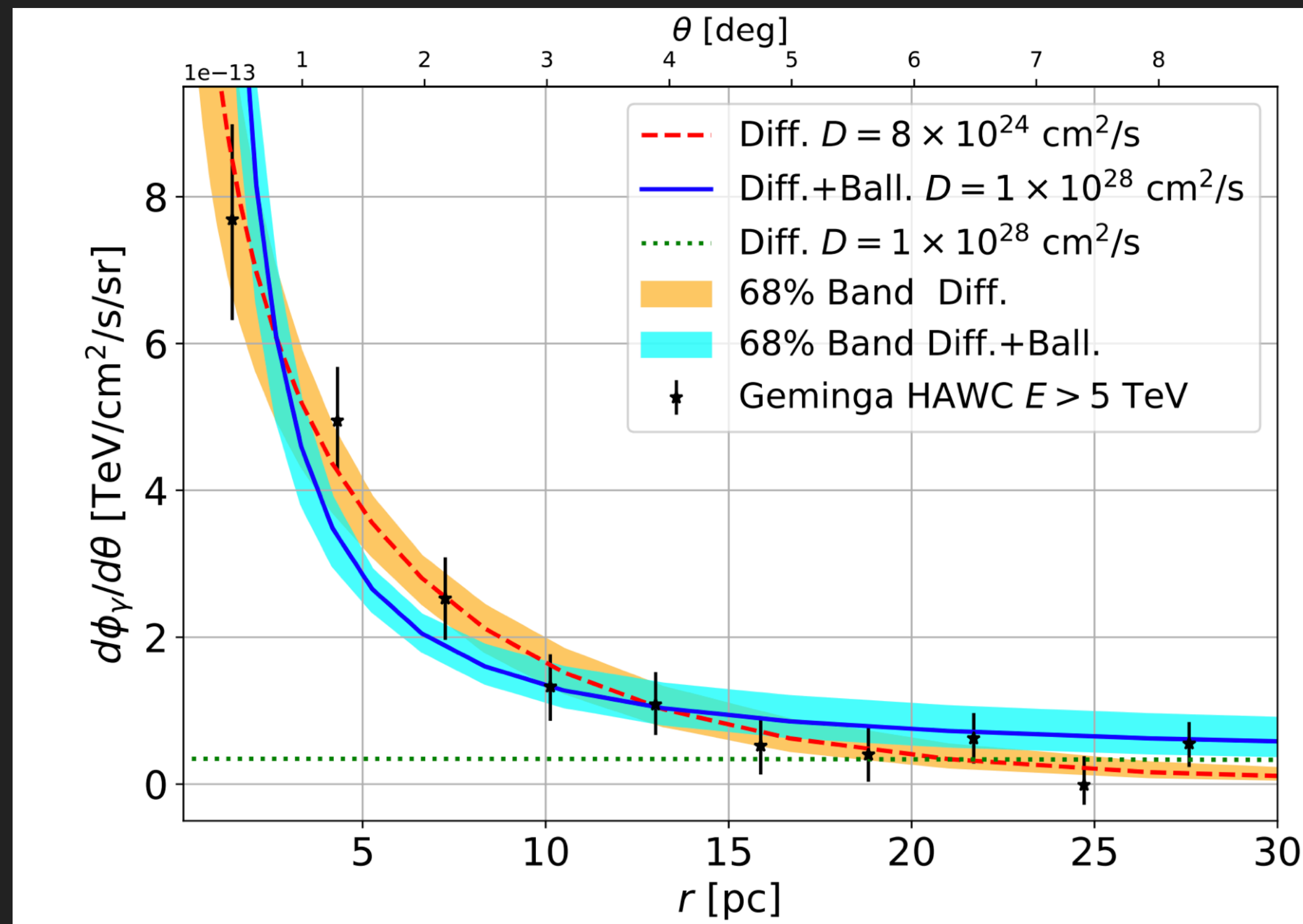


TAKING A DEEPER DIVE INTO INHIBITED DIFFUSION

- ▶ By combining the large number of TeV halo observations along with energetic considerations – we know that local diffusion must be inhibited.

Recchia et al. (2021; 2106.02275)

Bao et al. (2021; 2107.07395)



$$\frac{\partial W}{\partial t} + v_A \frac{\partial W}{\partial z} = (\Gamma_{CR} + \Gamma_{NLD}) W(k, z, t)$$

$$\Gamma_{CR}(k) = \frac{2\pi}{3} \frac{c |v_\alpha|}{k W(k)} \left(\frac{B_0^2}{8\pi} \right)^{-1} \left[p^4 \frac{\partial f}{\partial z} \right]_{p_{\text{res}}}$$

$$\Gamma_{NLD}(k) = c_k v_\alpha \begin{cases} k^{3/2} W^{1/2} & \text{Kolmogorov} \\ k^2 W & \text{Kraichnan} \end{cases}$$

$$D(p, t) = \frac{4}{3\pi} \frac{cr_L(p)}{k_{\text{res}} W(z, k_{\text{res}})}$$

TEV HALOS SOLVE COSMIC-RAY DIFFUSION

- ▶ Many uncertainties in these models:
 - ▶ Role of Supernova Remnant
 - ▶ Disruption by molecular gas or magnetic fields
 - ▶ Pulsar Proper Motion
 - ▶ 1D vs. 3D diffusion
 - ▶ non-Resonant Terms
 - ▶ Halos in close proximity

Possible origin of the slow-diffusion region around Geminga

Kun Fang^{1*} Xiao-Jun Bi^{1,2†} Peng-Fei Yin^{1‡}

¹ Key Laboratory of Particle Astrophysics, Institute of High Energy Physics, Chinese Academy of Sciences, Beijing 100049, China

² School of Physical Sciences, University of Chinese Academy of Sciences, Beijing 100049, China

23 July 2019

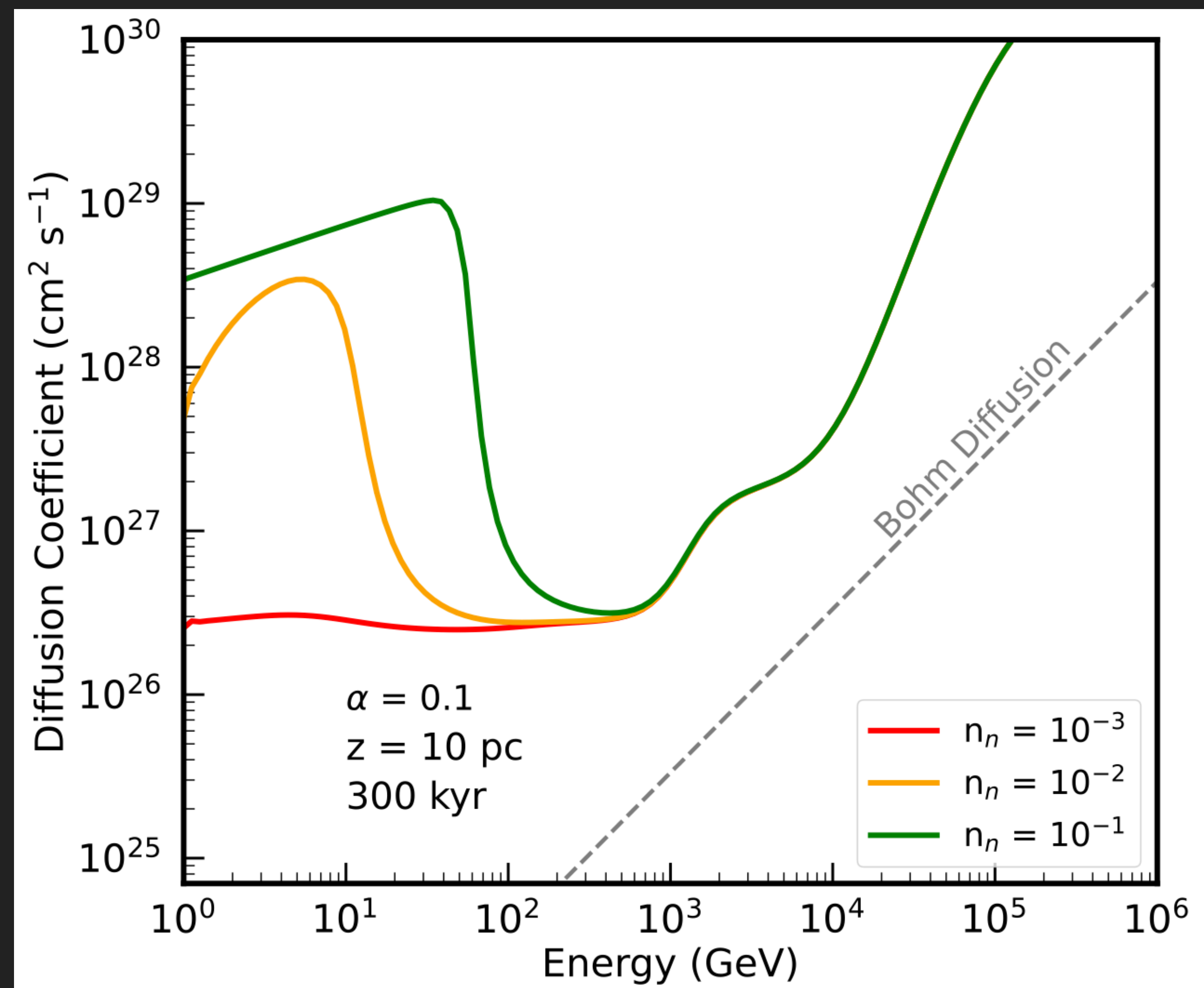
ABSTRACT

Geminga pulsar is surrounded by a multi-TeV γ -ray halo radiated by the high energy electrons and positrons accelerated by the central pulsar wind nebula (PWN). The angular profile of the γ -ray emission reported by HAWC indicates an anomalously slow diffusion for the cosmic-ray electrons and positrons in the halo region around Geminga. In the paper we study the possible mechanism for the origin of the slow diffusion. At first, we consider the self-generated Alfvén waves due to the streaming instability of the electrons and positrons released by Geminga. However, even considering a very optimistic scenario for the wave growth, we find this mechanism DOES NOT work to account for the extremely slow diffusion at the present day if taking the proper motion of Geminga pulsar into account. The reason is straightforward as the PWN is too weak to generate enough high energy electrons and positrons to stimulate strong turbulence at the late time. We then propose an assumption that the strong turbulence is generated by the shock wave of the parent supernova remnant (SNR) of Geminga. Geminga may still be inside the SNR, and we find that the SNR can provide enough energy to generate the slow-diffusion circumstance. The TeV halos around PSR B0656+14, Vela X, and PSR J1826-1334 may also be explained under this assumption.

Key words: cosmic rays – ISM: individual objects: Geminga nebula – ISM: supernova remnants – turbulence

106421v3 [astro-ph.HE] 22 Jul 2019

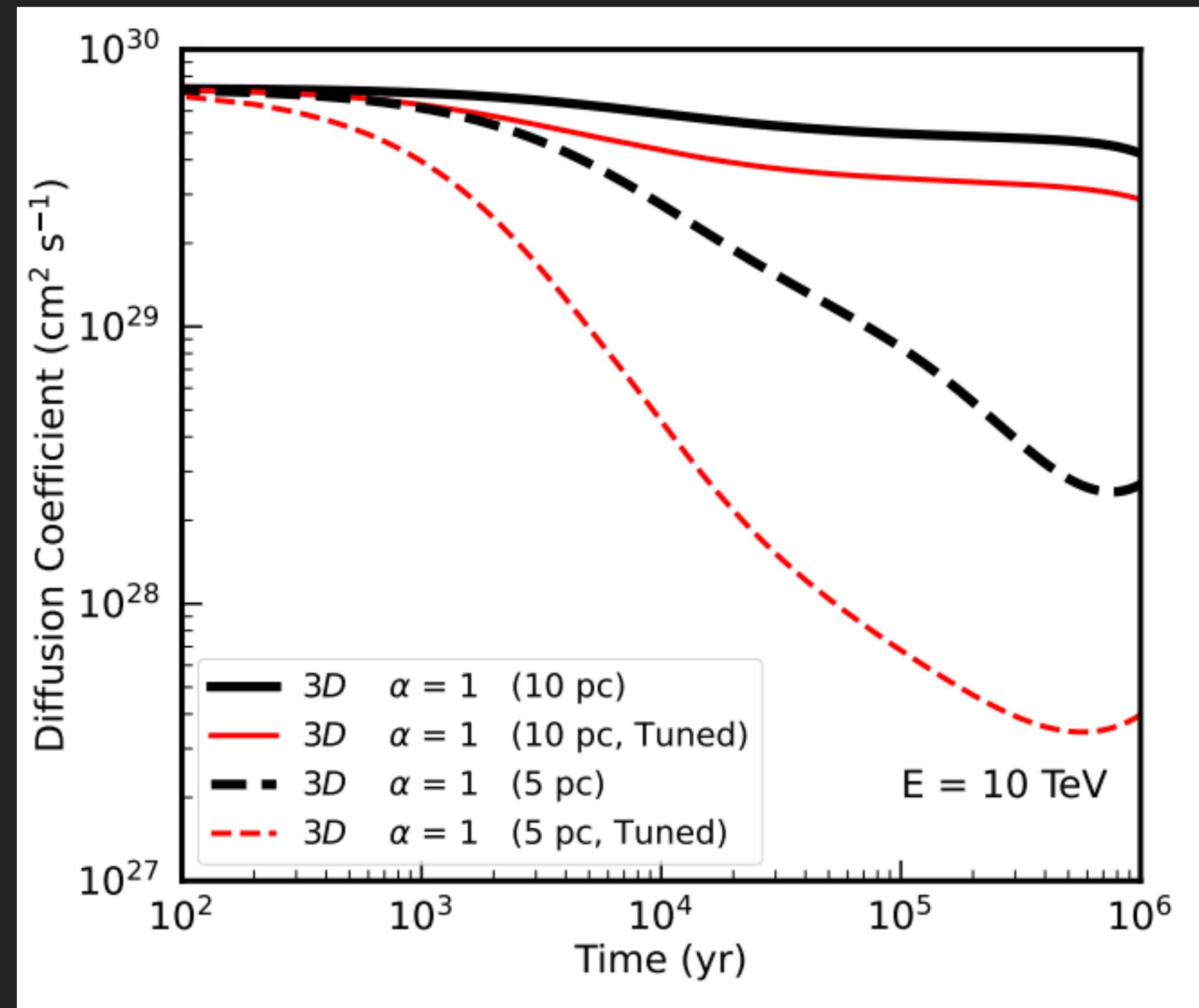
- ▶ Many uncertainties in these models:
 - ▶ Role of Supernova Remnant
 - ▶ Disruption by molecular gas or magnetic fields
 - ▶ Pulsar Proper Motion
 - ▶ 1D vs. 3D diffusion
 - ▶ non-Resonant Terms
 - ▶ Halos in close proximity



- ▶ Many uncertainties in these models:
 - ▶ Role of Supernova Remnant
 - ▶ Disruption by molecular gas or magnetic fields
 - ▶ Pulsar Proper Motion
 - ▶ 1D vs. 3D diffusion
 - ▶ non-Resonant Terms
 - ▶ Halos in close proximity



- ▶ Many uncertainties in these models:
 - ▶ Role of Supernova Remnant
 - ▶ Disruption by molecular gas or magnetic fields
 - ▶ Pulsar Proper Motion
 - ▶ 1D vs. 3D diffusion
 - ▶ non-Resonant Terms
 - ▶ Halos in close proximity



- ▶ Many uncertainties in these models:
 - ▶ Role of Supernova Remnant
 - ▶ Disruption by molecular gas or magnetic fields
 - ▶ Pulsar Proper Motion
 - ▶ 1D vs. 3D diffusion
 - ▶ non-Resonant Terms
 - ▶ Halos in close proximity



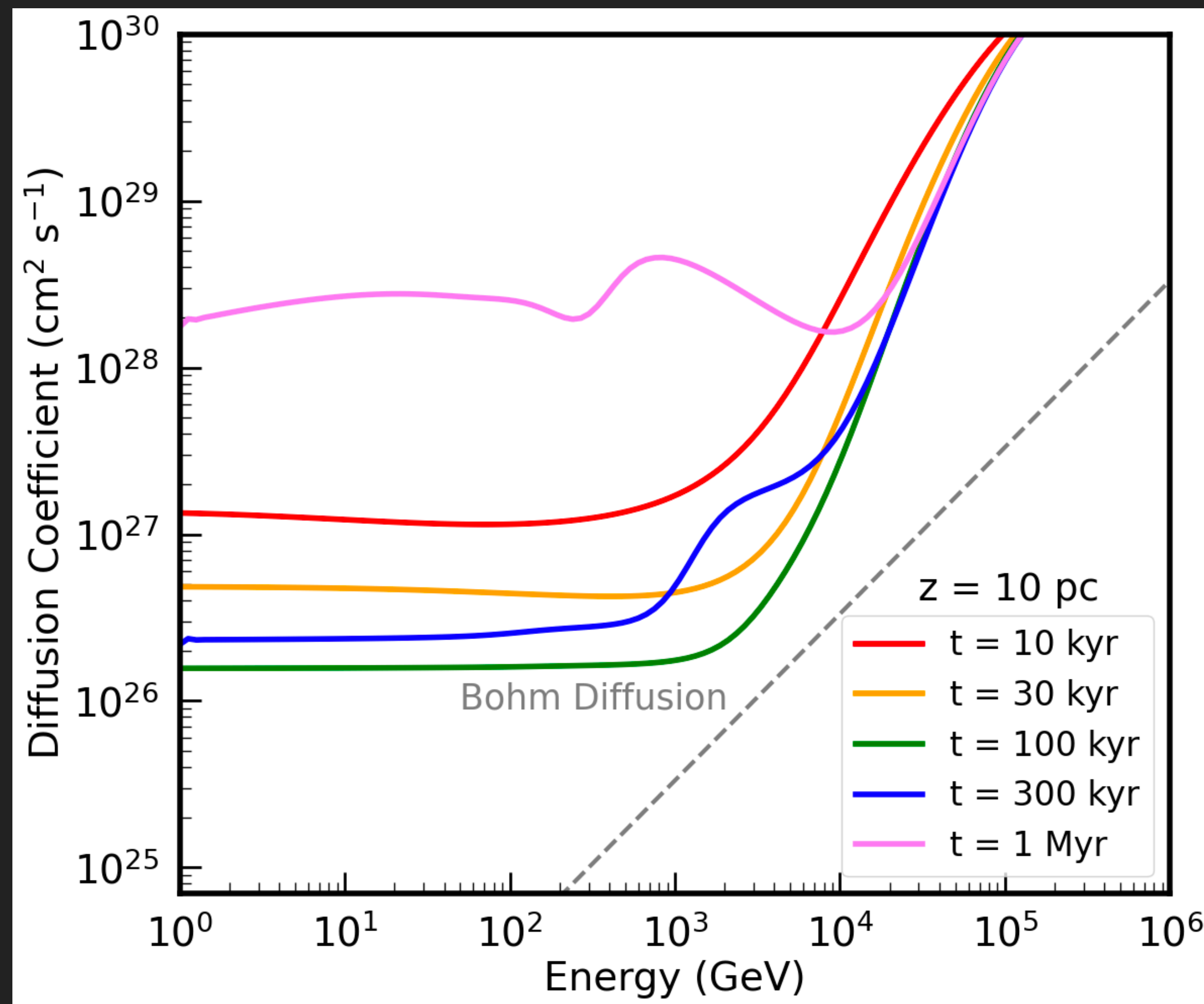
- ▶ Many uncertainties in these models:
 - ▶ Role of Supernova Remnant
 - ▶ Disruption by molecular gas or magnetic fields
 - ▶ Pulsar Proper Motion
 - ▶ 1D vs. 3D diffusion
 - ▶ non-Resonant Terms
 - ▶ Halos in close proximity



TEV HALOS SOLVE COSMIC-RAY DIFFUSION

Evoli, TL, Morlino (2018; 1807.09263)
Mukhopadhyay & TL (2021; 2111.01143)

- ▶ Several Predictions of these Models:
 - ▶ Relatively flat low-energy diffusion coefficient.
 - ▶ Highly energy dependent diffusion coefficient at high energies.



Kinetic simulations of electron-positron induced streaming instability in the context of gamma-ray halos around pulsars

Illya Plotnikov ¹, Allard Jan van Marle ², Claire Guépin ², Alexandre Marcowith ², and Pierrick Martin ¹

¹ IRAP, CNRS, OMP, Université de Toulouse III – Paul Sabatier, Toulouse, France
e-mail: illya.plotnikov@irap.omp.eu

² Laboratoire Univers et Particules de Montpellier (LUPM), Université de Montpellier, CNRS/IN2P3, CC72, Place Eugène Bataillon, F-34095 Montpellier Cedex 5, France

Received Month XX, 2024; accepted Month XX, 2024

ABSTRACT

Context. The possibility of slow diffusion regions as the origin for extended TeV emission halos around some pulsars (such as PSR J0633+1746 and PSR B0656+14) challenges the standard scaling of the electron diffusion coefficient in the interstellar medium.

Aims. Self-generated turbulence by electron-positron pairs streaming out of the pulsar wind nebula was proposed as a possible mechanism to produce the enhanced turbulence required to explain the morphology and brightness of these TeV halos.

Methods. We perform fully kinetic 1D3V particle-in-cell simulations of this instability, considering the case where streaming electrons and positrons have the same density. This implies purely resonant instability as the beam does not carry any current.

Results. We compare the linear phase of the instability with analytical theory and find very reasonable agreement. The non-linear phase of the instability is also studied, which reveals that the intensity of saturated waves is consistent with a momentum exchange criterion between a decelerating beam and growing magnetic waves. With the adopted parameters, the instability-driven wavemodes cover both the Alfvénic (fluid) and kinetic scales. The spectrum of the produced waves is non-symmetric, with left-handed circular polarisation waves being strongly damped when entering the ion-cyclotron branch, while right-handed waves are suppressed at smaller wavelength when entering the Whistler branch. The low-wavenumber part of the spectrum remains symmetric when in the Alfvénic branch. As a result, positrons behave dynamically differently compared to electrons. The final drift velocity of positrons can maintain a larger value than the ambient Alfvén speed V_A while the drift of electrons can drop below V_A . We also observed a second harmonic plasma emission in the wave spectrum. An MHD-PIC approach is warranted to probe hotter beams and investigate the Alfvén branch physics. We provide a few such test simulations to support this assertion.

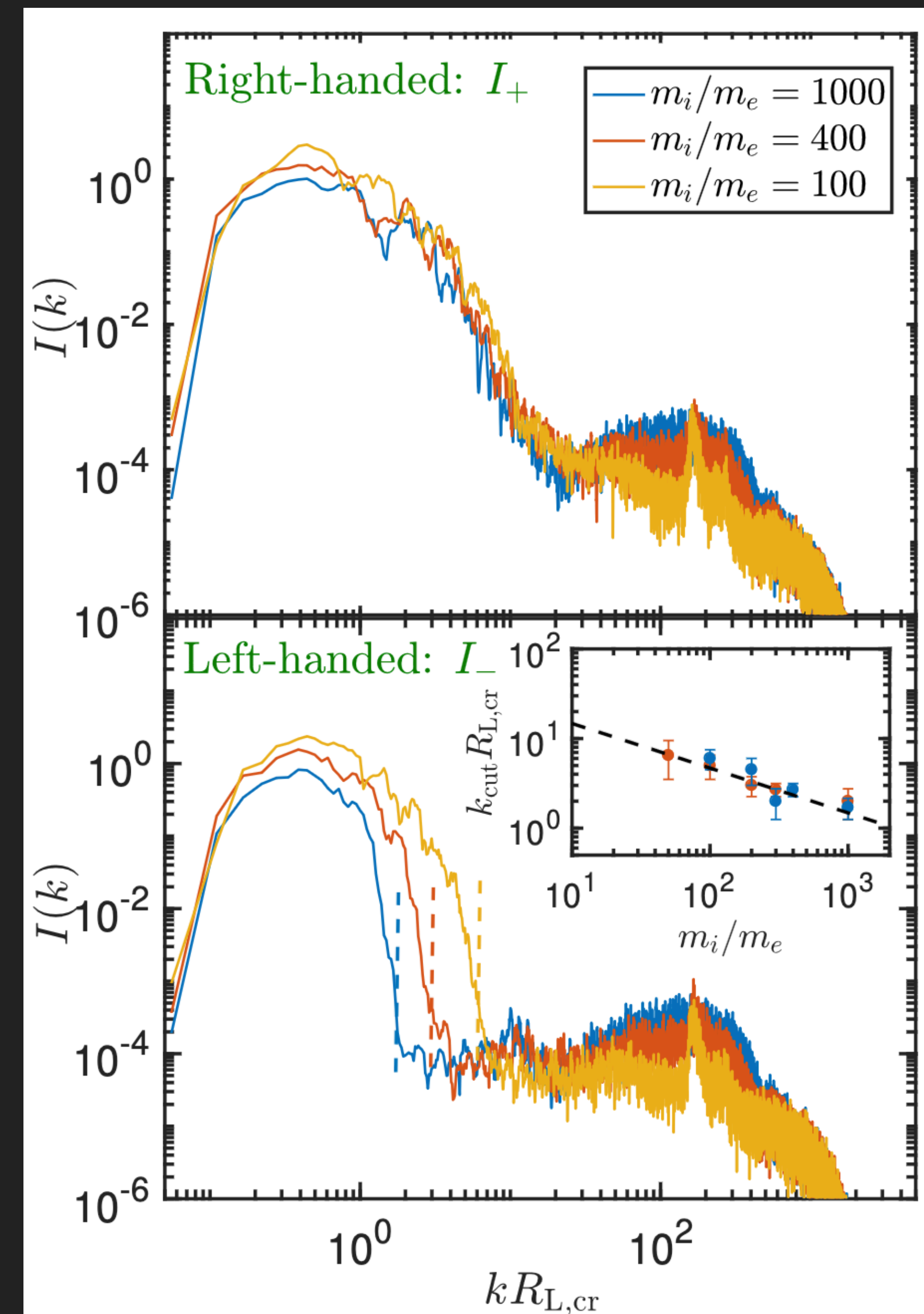
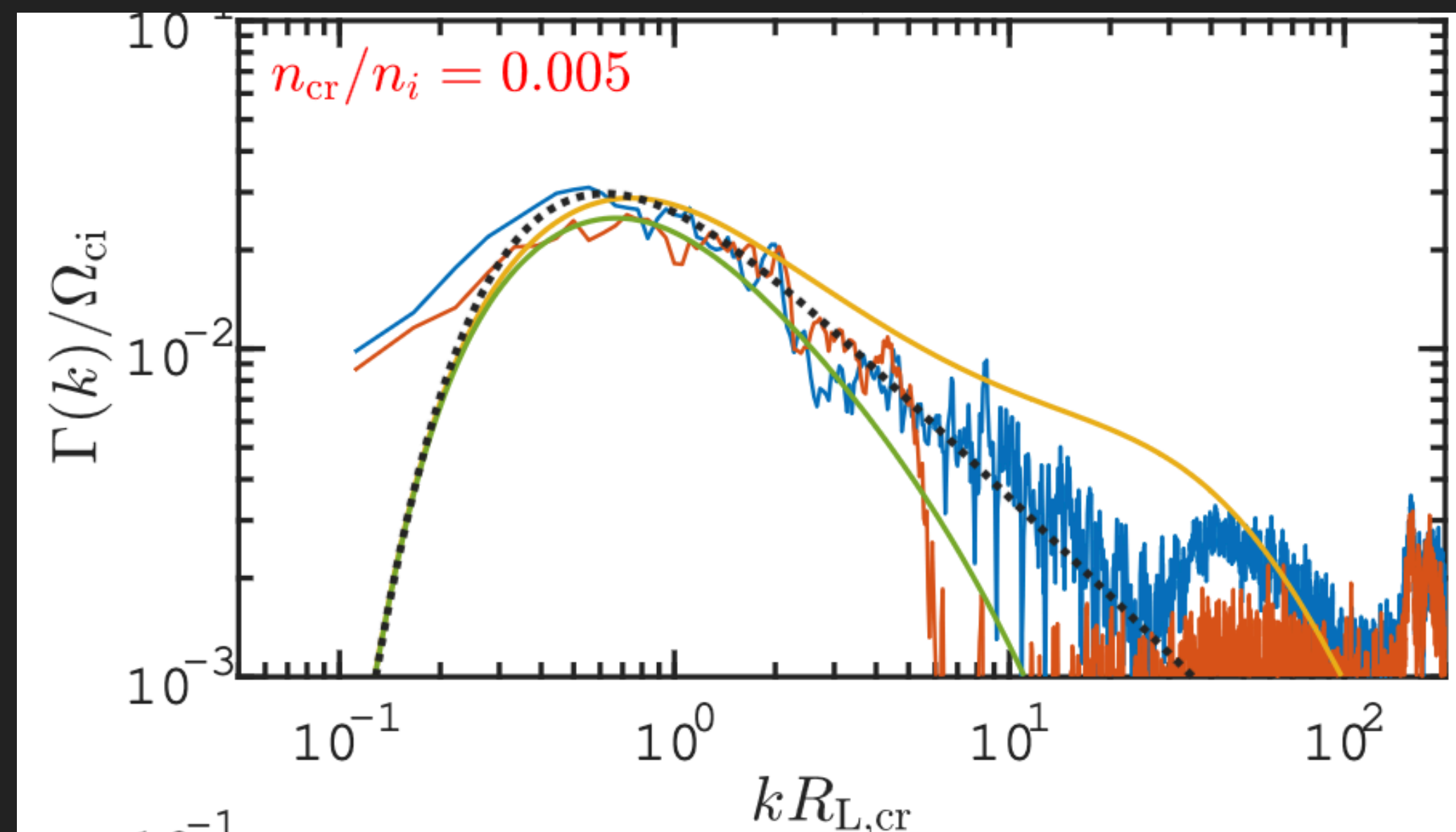
Conclusions. This work confirms that the self-confinement scenario develops essentially according to analytical expectations, but some of the adopted approximations (like the distribution of non-thermal particles in the beam) need to be revised and other complementary numerical techniques should be used to get closer to more realistic configuration.

Key words. Pulsars:general – Instabilities – Plasmas – Methods: numerical

CONFIRMATION FROM SIMULATIONS

Plotnikov et al. (2024; 2406.02945)

- ▶ Results in the linear regime are consistent between PIC simulations and analytic models
- ▶ In non-linear regime - several new effects
 - ▶ Difference between right-handed and left-handed waves in an ionic background causes positrons to propagate faster than electrons.



Kinetic simulations of electron-positron induced streaming instability in the context of gamma-ray halos around pulsars

Illya Plotnikov ¹, Allard Jan van Marle ², Claire Guépin ², Alexandre Marcowith ², and Pierrick Martin ¹

¹ IRAP, CNRS, OMP, Université de Toulouse III – Paul Sabatier, Toulouse, France
e-mail: illya.plotnikov@irap.omp.eu

² Laboratoire Univers et Particules de Montpellier (LUPM), Université de Montpellier, CNRS/IN2P3, CC72, Place Eugène Bataillon, F-34095 Montpellier Cedex 5, France

Received Month XX, 2024; accepted Month XX, 2024

ABSTRACT

Context. The possibility of slow diffusion regions as the origin for extended TeV emission halos around some pulsars (such as PSR J0633+1746 and PSR B0656+14) challenges the standard scaling of the electron diffusion coefficient in the interstellar medium.

Aims. Self-generated turbulence by electron-positron pairs streaming out of the pulsar wind nebula was proposed as a possible mechanism to produce the enhanced turbulence required to explain the morphology and brightness of these TeV halos.

Methods. We perform fully kinetic 1D3V particle-in-cell simulations of this instability, considering the case where streaming electrons and positrons have the same density. This implies purely resonant instability as the beam does not carry any current.

Results. We compare the linear phase of the instability with analytical theory and find very reasonable agreement. The non-linear phase of the instability is also studied, which reveals that the intensity of saturated waves is consistent with a momentum exchange criterion between a decelerating beam and growing magnetic waves. With the adopted parameters, the instability-driven wavemodes cover both the Alfvénic (fluid) and kinetic scales. The spectrum of the produced waves is non-symmetric, with left-handed circular polarisation waves being strongly damped when entering the ion-cyclotron branch, while right-handed waves are suppressed at smaller wavelength when entering the Whistler branch. The low-wavenumber part of the spectrum remains symmetric when in the Alfvénic branch. As a result, positrons behave dynamically differently compared to electrons. The final drift velocity of positrons can maintain a larger value than the ambient Alfvén speed V_A while the drift of electrons can drop below V_A . We also observed a second harmonic plasma emission in the wave spectrum. An MHD-PIC approach is warranted to probe hotter beams and investigate the Alfvén branch physics. We provide a few such test simulations to support this assertion.

Conclusions. This work confirms that the self-confinement scenario develops essentially according to analytical expectations, but some of the adopted approximations (like the distribution of non-thermal particles in the beam) need to be revised and other complementary numerical techniques should be used to get closer to more realistic configuration.

Key words. Pulsars:general – Instabilities – Plasmas – Methods: numerical

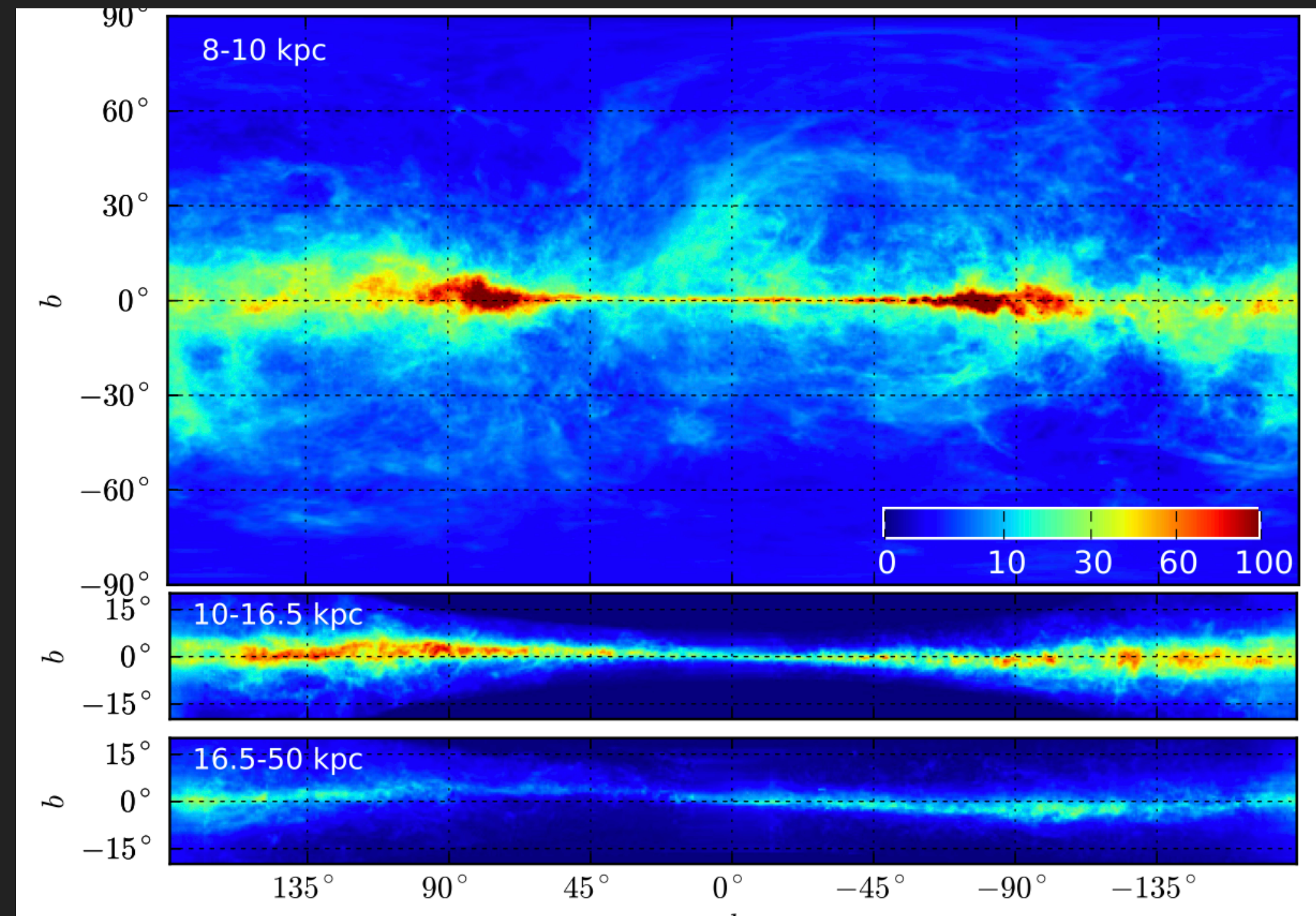


THE FUTURE: THE PROMISE OF TEV HALOS FOR DIFFUSE EMISSION STUDIES

- ▶ High Angular Resolution
- ▶ Long energy-lever arm (20 GeV – 100 TeV)
- ▶ Bifurcation in electron/proton morphology
 - ▶ $D_{\text{proton}} \propto E^{\delta/2}$
 - ▶ $D_{\text{electron}} \propto E^{\delta/2-1}$

NEED MODELS IN ORDER TO USE THESE OBSERVATIONS TO UNDERSTAND PHYSICS

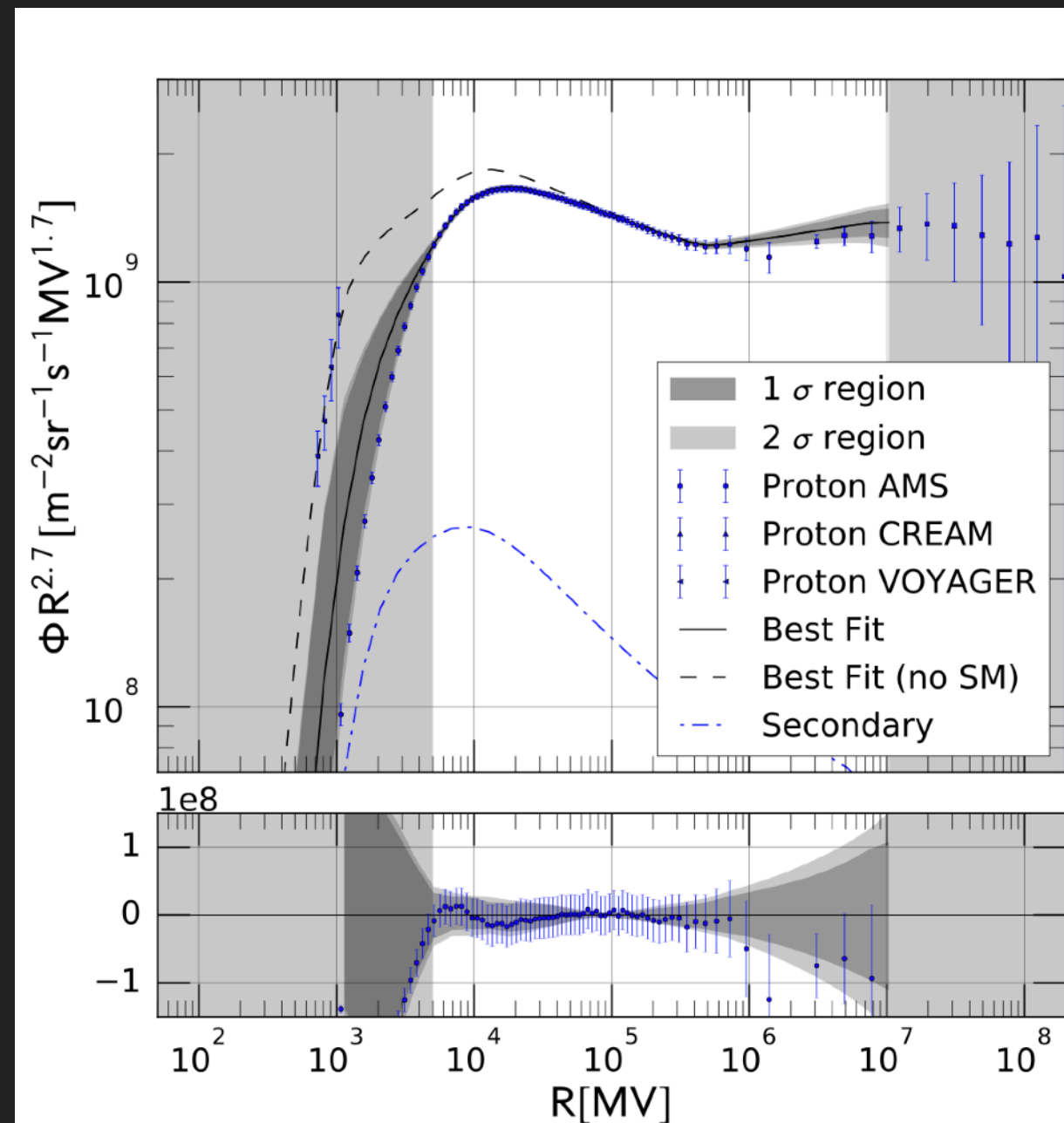
$$\begin{aligned}
 \underbrace{\frac{\partial \psi(\vec{r}, p, t)}{\partial t}}_{\text{flux}} &= \underbrace{Q(\vec{r}, p, t)}_{\text{source}} + \underbrace{\vec{\nabla} \times (D_{xx} \vec{\nabla} \psi)}_{\text{diffusion}} - \underbrace{\vec{V} \psi}_{\text{convection}} + \underbrace{\frac{\partial}{\partial p} p^2 D_{pp} \frac{\partial}{\partial p^2} \psi}_{\text{re-acceleration}} \\
 &\quad - \underbrace{\frac{\partial}{\partial p} \left(\dot{p} \psi - \frac{p}{3} (\vec{\nabla} \times \vec{V}) \psi \right)}_{\text{energy loss}} - \underbrace{\frac{\psi}{\tau_f}}_{\text{fragmentation}} - \underbrace{\frac{\psi}{\tau_r}}_{\text{radioactive decay}}
 \end{aligned}$$




TEV HALOS BREAK GEV GAMMA-RAY DIFFUSE EMISSION MODELS

Korsmeier & Cuoco (2016; 1607.06093)

Fit parameters	(uni-PHe)	(uni-PHePbar)	(P)	(PHe)	(main)	(diMauro)	(1GV)	(noVc-1GV)	(noVc-5GV)
$\gamma_{1,p}$	-	-	$1.52^{+0.21}_{-0.32}$	$1.27^{+0.11}_{-0.07}$	$1.36^{+0.07}_{-0.10}$	$1.38^{+0.07}_{-0.10}$	$1.32^{+0.05}_{-0.12}$	$1.61^{+0.06}_{-0.10}$	$1.76^{+0.07}_{-0.04}$
$\gamma_{2,p}$	-	-	$2.52^{+0.12}_{-0.45}$	$2.069^{+0.098}_{-0.069}$	$2.493^{+0.010}_{-0.026}$	$2.499^{+0.026}_{-0.014}$	$2.455^{+0.014}_{-0.007}$	$2.421^{+0.010}_{-0.014}$	$2.454^{+0.026}_{-0.014}$
γ_1	$1.92^{+0.08}_{-0.14}$	$1.50^{+0.07}_{-0.12}$	-	$1.53^{+0.24}_{-0.11}$	$1.29^{+0.04}_{-0.09}$	$1.26^{+0.10}_{-0.06}$	$1.32^{+0.06}_{-0.12}$	$1.65^{+0.07}_{-0.11}$	$1.70^{+0.06}_{-0.07}$
γ_2	$2.582^{+0.010}_{-0.034}$	$2.404^{+0.006}_{-0.022}$	-	$2.003^{+0.094}_{-0.003}$	$2.440^{+0.006}_{-0.018}$	$2.451^{+0.018}_{-0.010}$	$2.412^{+0.012}_{-0.006}$	$2.381^{+0.010}_{-0.010}$	$2.407^{+0.022}_{-0.014}$
R_0 [GV]	$8.16^{+1.22}_{-1.54}$	$8.79^{+1.17}_{-1.55}$	$4.38^{+3.23}_{-1.54}$	$10.5^{+1.40}_{-1.59}$	$5.54^{+0.76}_{-0.54}$	$5.44^{+0.54}_{-0.54}$	$5.52^{+0.33}_{-0.83}$	$7.01^{+0.98}_{-0.54}$	$8.63^{+0.98}_{-0.76}$
s	$0.32^{+0.08}_{-0.02}$	$0.41^{+0.09}_{-0.07}$	$0.48^{+0.16}_{-0.31}$	$0.59^{+0.16}_{-0.04}$	$0.50^{+0.02}_{-0.04}$	$0.50^{+0.05}_{-0.03}$	$0.43^{+0.04}_{-0.03}$	$0.31^{+0.03}_{-0.03}$	$0.32^{+0.04}_{-0.05}$
δ	$0.16^{+0.03}_{-0.02}$	$0.36^{+0.04}_{-0.03}$	$0.29^{+0.46}_{-0.18}$	$0.72^{+0.01}_{-0.11}$	$0.28^{+0.03}_{-0.01}$	$0.27^{+0.02}_{-0.04}$	$0.32^{+0.03}_{-0.02}$	$0.40^{+0.01}_{-0.01}$	$0.36^{+0.02}_{-0.02}$
D_0 [10^{28} cm ² /s]	$2.77^{+2.95}_{-0.53}$	$2.83^{+0.90}_{-0.50}$	$4.78^{+5.22}_{-3.49}$	$5.95^{+0.83}_{-1.37}$	$9.30^{+0.70}_{-5.48}$	$9.04^{+0.96}_{-3.95}$	$8.19^{+1.81}_{-4.68}$	$4.92^{+1.12}_{-2.36}$	$4.60^{+2.71}_{-2.04}$
v_A [km/s]	$6.80^{+1.18}_{-2.73}$	$29.2^{+2.80}_{-1.47}$	$21.2^{+38.8}_{-21.2}$	$1.84^{+2.36}_{-1.08}$	$20.2^{+3.26}_{-6.33}$	$18.2^{+3.15}_{-5.91}$	$25.0^{+0.92}_{-2.30}$	$22.8^{+1.46}_{-1.05}$	$20.7^{+1.14}_{-3.43}$
$v_{0,c}$ [km/s]	$40.9^{+59.1}_{-5.89}$	$40.2^{+38.1}_{-25.2}$	$5.82^{+94.2}_{-5.82}$	$87.8^{+12.2}_{-7.57}$	$69.7^{+22.0}_{-24.7}$	$57.3^{+41.1}_{-12.3}$	$44.0^{+8.4}_{-16.5}$	-	-
z_h [kpc]	$3.77^{+3.23}_{-1.77}$	$2.04^{+0.40}_{-0.04}$	$4.22^{+2.78}_{-2.22}$	$6.55^{+0.45}_{-1.63}$	$5.43^{+1.57}_{-3.43}$	$5.84^{+1.16}_{-3.84}$	$6.00^{+1.00}_{-4.00}$	$5.05^{+1.95}_{-3.05}$	$4.12^{+2.88}_{-2.12}$
ϕ_{AMS}	300^{+60}_{-80}	780^{+80}_{-40}	620^{+180}_{-195}	580^{+45}_{-115}	400^{+90}_{-40}	360^{+115}_{-45}	700^{+20}_{-50}	640^{+20}_{-20}	340^{+45}_{-125}



- Assume CR propagation is homogeneous.
- Fit data to local AMS-02 observables.

 Moon (To Scale)

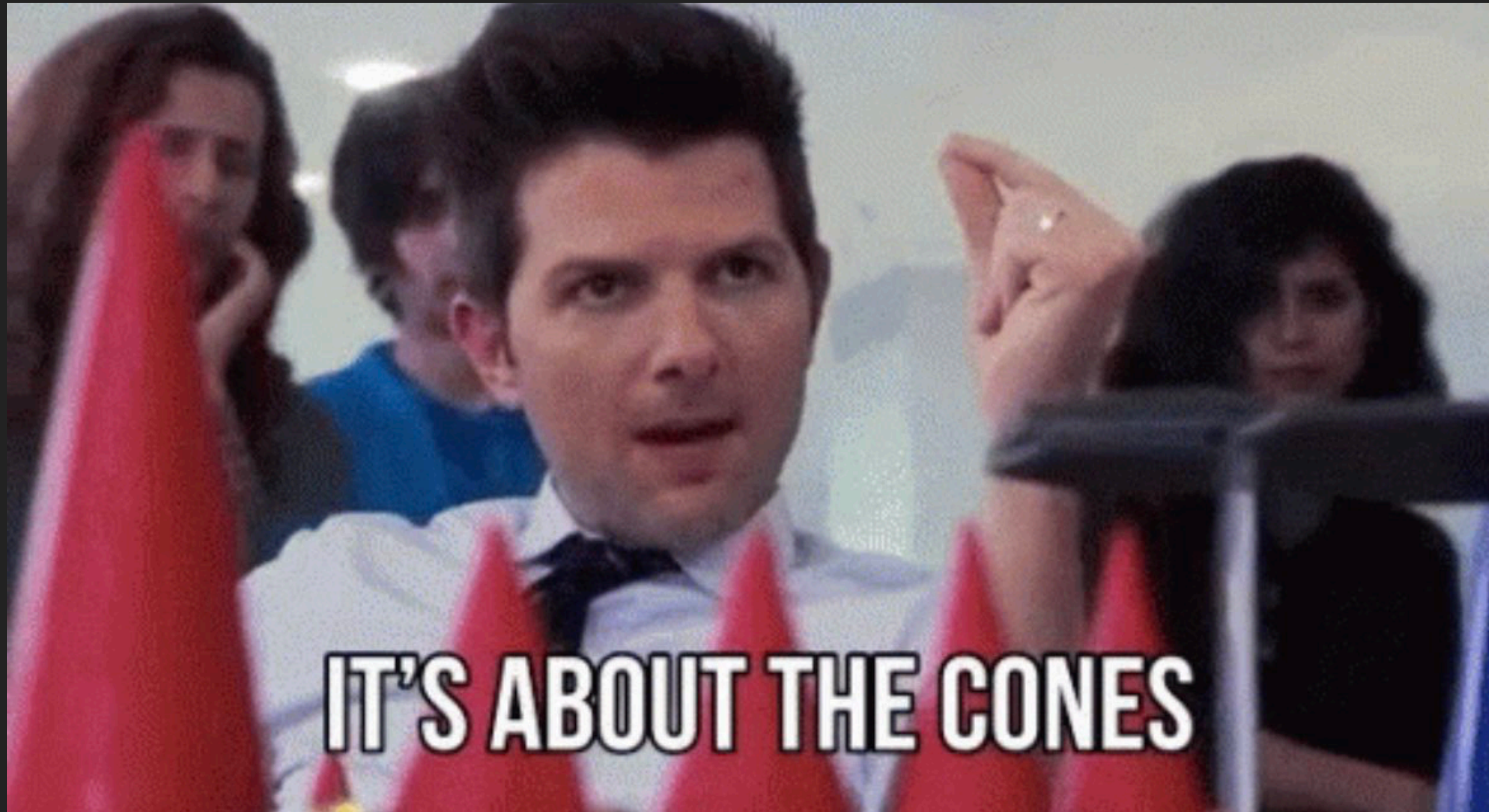
Geminga

PSR B0656+14

- But propagation is not homogeneous.
- Local TeV observations might not tell you anything!

USING TEV HALOS TO FIX COSMIC-RAY DIFFUSION MODELS

- ▶ It's about the sources.



TEV HALOS SOLVE COSMIC-RAY DIFFUSION

▶ Pulsar catalogs provide an answer:

▶ >3000 pulsars

▶ Specific locations, ages, and spin down powers

▶ Translates directly into local diffusion model in streaming instability models.

#	PSRJ	P0 (s)	P1	DIST (kpc)	AGE (Yr)	BSURF (G)	EDOT (ergs/s)
1	J0537-6910	0.016122	5.18e-14	49.700	4.93e+03	9.25e+11	4.88e+38
2	J0534+2200	0.033392	4.21e-13	2.000	1.26e+03	3.79e+12	4.46e+38
3	J0540-6919	0.050570	4.79e-13	49.700	1.67e+03	4.98e+12	1.46e+38
4	J1813-1749	0.044741	1.27e-13	4.700	5.58e+03	2.41e+12	5.60e+37
5	J1400-6325	0.031182	3.89e-14	7.000	1.27e+04	1.11e+12	5.07e+37
6	J1747-2809	0.052153	1.56e-13	8.141	5.31e+03	2.88e+12	4.33e+37
7	J1833-1034	0.061884	2.02e-13	4.100	4.85e+03	3.58e+12	3.37e+37
8	J2022+3842	0.048579	8.61e-14	10.000	8.94e+03	2.07e+12	2.96e+37
9	J0205+6449	0.065716	1.94e-13	3.200	5.37e+03	3.61e+12	2.70e+37
10	J2229+6114	0.051624	7.83e-14	3.000	1.05e+04	2.03e+12	2.25e+37
11	J1513-5908	0.151582	1.53e-12	4.400	1.57e+03	1.54e+13	1.73e+37
12	J1617-5055	0.069357	1.35e-13	4.743	8.13e+03	3.10e+12	1.60e+37
13	J1124-5916	0.135477	7.53e-13	5.000	2.85e+03	1.02e+13	1.19e+37
14	J1930+1852	0.136855	7.51e-13	7.000	2.89e+03	1.03e+13	1.16e+37
15	J1023-5746	0.111472	3.84e-13	2.080	4.60e+03	6.62e+12	1.09e+37
16	J1420-6048	0.068180	8.32e-14	5.632	1.30e+04	2.41e+12	1.04e+37
17	J1410-6132	0.050052	3.20e-14	13.510	2.48e+04	1.28e+12	1.01e+37
18	J1849-0001	0.038523	1.42e-14	*	4.31e+04	7.47e+11	9.78e+36
19	J1402+13	0.005890	4.83e-17	*	1.93e+06	1.71e+10	9.34e+36
20	J1846-0258	0.326571	7.11e-12	5.800	7.28e+02	4.88e+13	8.06e+36
21	J0835-4510	0.089328	1.25e-13	0.280	1.13e+04	3.38e+12	6.92e+36
22	J1811-1925	0.064667	4.40e-14	5.000	2.33e+04	1.71e+12	6.42e+36
23	J1111-6039	0.106670	1.95e-13	*	8.66e+03	4.62e+12	6.35e+36
24	J1813-1246	0.048072	1.76e-14	2.635	4.34e+04	9.30e+11	6.24e+36
25	J1838-0537	0.145708	4.72e-13	*	4.89e+03	8.39e+12	6.02e+36
26	J1838-0655	0.070498	4.92e-14	6.600	2.27e+04	1.89e+12	5.55e+36
27	J1418-6058	0.110573	1.69e-13	1.885	1.03e+04	4.38e+12	4.95e+36
28	J1935+2025	0.080118	6.08e-14	4.598	2.09e+04	2.23e+12	4.66e+36
29	J1856+0245	0.080907	6.21e-14	6.318	2.06e+04	2.27e+12	4.63e+36
30	J1112-6103	0.064962	3.15e-14	4.500	3.27e+04	1.45e+12	4.53e+36
31	J1640-4631	0.206443	9.76e-13	12.750	3.35e+03	1.44e+13	4.38e+36
32	J1844-0346	0.112855	1.55e-13	*	1.16e+04	4.23e+12	4.25e+36
33	J1952+3252	0.039531	5.84e-15	3.000	1.07e+05	4.86e+11	3.74e+36
34	J1826-1256	0.110224	1.21e-13	1.550	1.44e+04	3.70e+12	3.58e+36
35	J1709-4429	0.102459	9.30e-14	2.600	1.75e+04	3.12e+12	3.41e+36
36	J2021+3651	0.103741	9.57e-14	1.800	1.72e+04	3.19e+12	3.38e+36
37	J1524-5625	0.078219	3.90e-14	3.378	3.18e+04	1.77e+12	3.21e+36
38	J1357-6429	0.166108	3.60e-13	3.100	7.31e+03	7.83e+12	3.10e+36
39	J1913+1011	0.035909	3.37e-15	4.613	1.69e+05	3.52e+11	2.87e+36
40	J1826-1334	0.101487	7.53e-14	3.606	2.14e+04	2.80e+12	2.84e+36

Pulsar searches and timing with the square kilometre array

R. Smits¹, M. Kramer¹, B. Stappers¹, D. R. Lorimer^{2,3}, J. Cordes⁴, and A. Faulkner¹

¹ Jodrell Bank Centre for Astrophysics, University of Manchester, UK

e-mail: Roy.Smits@manchester.ac.uk

² Department of Physics, 210 Hodges Hall, West Virginia University, Morgantown, WV 26506, USA

³ National Radio Astronomy Observatory, Green Bank, USA

⁴ Astronomy Department, Cornell University, Ithaca, NY, USA

Received 13 June 2008 / Accepted 31 October 2008

ABSTRACT

The square kilometre array (SKA) is a planned multi purpose radio telescope with a collecting area approaching 1 million square metres. One of the key science objectives of the SKA is to provide exquisite strong-field tests of gravitational physics by finding and timing pulsars in extreme binary systems such as a pulsar-black hole binary. To find out how three preliminary SKA configurations will affect a pulsar survey, we have simulated SKA pulsar surveys for each configuration. We estimate that the total number of pulsars the SKA will detect, is around 14 000 normal pulsars and 6000 millisecond pulsars, using only the 1-km core and 30-min integration time. We describe a simple strategy for follow-up timing observations and find that, depending on the configuration, it would take 1–6 days to obtain a single timing point for 14 000 pulsars. Obtaining one timing point for the high-precision timing projects of the SKA, will take less than 14 h, 2 days, or 3 days, depending on the configuration. The presence of aperture arrays will be of great benefit here. We also study the computational requirements for beam forming and data analysis for a pulsar survey. Beam forming of the full field of view of the single pixel feed 15 m dishes using the 1 km core of the SKA requires about 2.2×10^{15} operations

CONCLUSIONS - TEV GAMMA-RAY MODELING

- ▶ TeV halos are a common feature around middle-aged (and possibly young and recycled pulsars).
- ▶ Understanding the earliest stages of TeV halo formation (or composite sources, if you prefer), is critical for understanding TeV halo evolution.
- ▶ TeV halos provide critical information that will be necessary to make detailed TeV emission models.